

Linear interpolation method in ensemble Kohn-Sham and range-separated density-functional approximations for excited states

Bruno Senjean,¹ Stefan Knecht,² Hans Jørgen Aa. Jensen,³ and Emmanuel Fromager^{1,*}

¹*Laboratoire de Chimie Quantique, Institut de Chimie, CNRS/Université de Strasbourg, 1 rue Blaise Pascal, F-67000 Strasbourg, France*

²*Laboratory of Physical Chemistry, ETH Zürich, Vladimir-Prelog Weg 2, CH-8093 Zürich, Switzerland*

³*Department of Physics, Chemistry and Pharmacy, University of Southern Denmark, Campusvej 55, DK-5230 Odense M, Denmark*

(Received 24 April 2015; published 24 July 2015)

Gross-Oliveira-Kohn density-functional theory (GOK-DFT) for ensembles is, in principle, very attractive but has been hard to use in practice. A practical model based on GOK-DFT for the calculation of electronic excitation energies is discussed. The model relies on two modifications of GOK-DFT: use of range separation and use of the slope of the linearly interpolated ensemble energy, rather than orbital energies. The range-separated approach is appealing, as it enables the rigorous formulation of a multideterminant state-averaged DFT method. In the exact theory, the short-range density functional, which complements the long-range wave-function-based ensemble energy contribution, should vary with the ensemble weights even when the density is held fixed. This weight dependence ensures that the range-separated ensemble energy varies linearly with the ensemble weights. When the (weight-independent) ground-state short-range exchange-correlation functional is used in this context, curvature appears, thus leading to an approximate weight-dependent excitation energy. In order to obtain unambiguous approximate excitation energies, we propose to interpolate linearly the ensemble energy between equiensembles. It is shown that such a linear interpolation method (LIM) can be rationalized and that it effectively introduces weight dependence effects. As proof of principle, the LIM has been applied to He, Be, and H₂ in both equilibrium and stretched geometries as well as the stretched HeH⁺ molecule. Very promising results have been obtained for both single (including charge transfer) and double excitations with spin-independent short-range local and semilocal functionals. Even at the Kohn-Sham ensemble DFT level, which is recovered when the range-separation parameter is set to 0, LIM performs better than standard time-dependent DFT.

DOI: [10.1103/PhysRevA.92.012518](https://doi.org/10.1103/PhysRevA.92.012518)

PACS number(s): 31.15.eg, 31.15.ee, 31.15.vj

I. INTRODUCTION

The standard approach for modeling excited states in the framework of density-functional theory (DFT) is the time-dependent (TD) linear response regime [1]. Despite its success, due to its low computational cost and relatively good accuracy, standard TD-DFT still suffers from various deficiencies, one of them being the absence of multiple excitations in the spectrum. This is directly connected with the so-called adiabatic approximation, which consists in using a frequency-independent exchange-correlation (xc) kernel in the linear response equations. In order to overcome such limitations, the combination of TD-DFT with density-matrix-based [2] or wave-function-based [3–5] methods by means of range separation has been investigated recently.

In this work, we propose to explore a time-independent range-separated DFT approach for excited states that is based on ensembles [6,7]. One of the motivations is the need for cheaper (in terms of computational cost) yet still reliable (in terms of accuracy) alternatives to standard second-order complete active space (CASPT2) [8] or *N*-electron valence state (NEVPT2) [9,10] perturbation theories for modeling, for example, photochemical processes [11,12]. Ensemble range-separated DFT was initially formulated by Pastorczak *et al.* [13]. The authors considered the particular case of Boltzmann ensemble weights. The latter were controlled by an effective temperature that can be used as a tunable parameter, in addition to the range-separation one. As shown in Ref. [14],

an exact adiabatic connection formula can be derived for the complementary short-range xc energy of an ensemble. Exactly as in the Kohn-Sham (KS) ensemble DFT [7,15,16], which is also referred to as the Gross-Oliveira-Kohn DFT (GOK-DFT), the variation of the short-range xc density functional with the ensemble weights plays a crucial role in the calculation of excitation energies [14]. So far, short-range density-functional approximations have been developed only for the ground state, not for ensembles. Consequently, an approximate (weight-independent) ground-state functional was used in Ref. [13].

The weight dependence of the range-separated ensemble energy and the ambiguity in the definition of an approximate excitation energy, which may become weight dependent when approximate functionals are used, is analyzed analytically and numerically in this work. By analogy with the fundamental gap problem [17], a simple and general linear interpolation method (LIM) is proposed and interpreted for the purpose of defining unambiguously approximate weight-independent excitation energies. The method becomes exact if exact functionals and wave functions are used. The paper is organized as follows: After a brief introduction to ground-state range-separated DFT in Sec. II A, the GOK-DFT is presented in Sec. II B and its exact range-separated extension is formulated in Sec. II C. The weight-independent density-functional approximation (WIDFA) is then discussed in detail for a two-state ensemble. The LIM is introduced in Sec. II D and rationalized in Sec. II E. The particular case of an approximate range-separated ensemble energy that is quadratic in the ensemble weight is then treated in Sec. II F. Comparison is made with Ref. [13] and TD adiabatic linear response theory in Sec. II G. A generalization to higher excitations is then given in Sec. II H.

*fromagere@unistra.fr

After the computational details in Sec. III, results obtained for He, Be, H₂, and HeH⁺ are presented and discussed in Sec. IV. We conclude this work with a summary in Sec. V.

II. THEORY

A. Range-separated density-functional theory for the ground state

According to the Hohenberg-Kohn theorem [18], the exact ground-state energy of an electronic system can be obtained variationally as

$$E_0 = \min_n \left\{ F[n] + \int d\mathbf{r} v_{\text{ne}}(\mathbf{r}) n(\mathbf{r}) \right\}, \quad (1)$$

where $v_{\text{ne}}(\mathbf{r})$ is the nuclear potential and the minimization is performed over electron densities $n(\mathbf{r})$ that integrate to a fixed number N of electrons. The universal Levy-Lieb (LL) functional [19] equals

$$F[n] = \min_{\Psi \rightarrow n} \langle \Psi | \hat{T} + \hat{W}_{\text{ee}} | \Psi \rangle, \quad (2)$$

where \hat{T} and $\hat{W}_{\text{ee}} \equiv \sum_{i < j}^N 1/r_{ij}$ are the kinetic energy and regular two-electron repulsion operators, respectively. Following Savin [20], we consider the decomposition of the latter into long- and short-range contributions,

$$\begin{aligned} 1/r_{12} &= w_{\text{ee}}^{\text{lr},\mu}(r_{12}) + w_{\text{ee}}^{\text{sr},\mu}(r_{12}), \\ w_{\text{ee}}^{\text{lr},\mu}(r_{12}) &= \text{erf}(\mu r_{12})/r_{12}, \end{aligned} \quad (3)$$

where erf is the error function and μ is a parameter in $[0, +\infty[$ that controls the range separation, thus leading to the partitioning

$$F[n] = F^{\text{lr},\mu}[n] + E_{\text{Hxc}}^{\text{sr},\mu}[n], \quad (4)$$

with

$$F^{\text{lr},\mu}[n] = \min_{\Psi \rightarrow n} \langle \Psi | \hat{T} + \hat{W}_{\text{ee}}^{\text{lr},\mu} | \Psi \rangle, \quad (5)$$

and $\hat{W}_{\text{ee}}^{\text{lr},\mu} \equiv \sum_{i < j}^N w_{\text{ee}}^{\text{lr},\mu}(r_{ij})$. The complementary μ -dependent short-range density-functional energy $E_{\text{Hxc}}^{\text{sr},\mu}[n]$ can be decomposed into Hartree (H) and xc terms, in analogy with conventional KS-DFT,

$$\begin{aligned} E_{\text{Hxc}}^{\text{sr},\mu}[n] &= E_{\text{H}}^{\text{sr},\mu}[n] + E_{\text{xc}}^{\text{sr},\mu}[n], \\ E_{\text{H}}^{\text{sr},\mu}[n] &= \frac{1}{2} \iint d\mathbf{r} d\mathbf{r}' n(\mathbf{r}) n(\mathbf{r}') w_{\text{ee}}^{\text{sr},\mu}(|\mathbf{r} - \mathbf{r}'|). \end{aligned} \quad (6)$$

Inserting Eq. (4) into Eq. (1) leads to the exact expression

$$\begin{aligned} E_0 &= \min_{\Psi} \left\{ \langle \Psi | \hat{T} + \hat{W}_{\text{ee}}^{\text{lr},\mu} + \hat{V}_{\text{ne}} | \Psi \rangle + E_{\text{Hxc}}^{\text{sr},\mu}[n_{\Psi}] \right\} \\ &= \langle \Psi_0^{\mu} | \hat{T} + \hat{W}_{\text{ee}}^{\text{lr},\mu} + \hat{V}_{\text{ne}} | \Psi_0^{\mu} \rangle + E_{\text{Hxc}}^{\text{sr},\mu}[n_{\Psi_0^{\mu}}], \end{aligned} \quad (7)$$

where $\hat{V}_{\text{ne}} = \int d\mathbf{r} v_{\text{ne}}(\mathbf{r}) \hat{n}(\mathbf{r})$ and $\hat{n}(\mathbf{r})$ is the density operator. The electron density obtained from the trial wave function Ψ is denoted n_{Ψ} . The exact minimizing wave function Ψ_0^{μ} in Eq. (7) has the same density n^0 as the physical fully interacting ground-state wave function Ψ_0 and it fulfills the self-consistent equation

$$\hat{H}^{\mu}[n_{\Psi_0^{\mu}}] | \Psi_0^{\mu} \rangle = \mathcal{E}_0^{\mu} | \Psi_0^{\mu} \rangle, \quad (8)$$

where

$$\hat{H}^{\mu}[n] = \hat{T} + \hat{W}_{\text{ee}}^{\text{lr},\mu} + \hat{V}_{\text{ne}} + \int d\mathbf{r} \frac{\delta E_{\text{Hxc}}^{\text{sr},\mu}[n]}{\delta n(\mathbf{r})} \hat{n}(\mathbf{r}). \quad (9)$$

It is readily seen from Eqs. (3) and (8) that the KS and Schrödinger equations are recovered in the limit of $\mu = 0$ and $\mu \rightarrow +\infty$, respectively. An exact combination of wave-function theory with KS-DFT is obtained in the range of $0 < \mu < +\infty$.

In order to perform practical range-separated DFT calculations, local and semilocal short-range density functionals have been developed in recent years [21–24]. In addition, various wave-function-theory-based methods have been adapted to this context in order to describe the long-range interaction: Hartree-Fock (HF) [25,26], second-order Møller-Plesset [25,27,28], the random-phase approximation [29,30], configuration interaction (CI) [31,32], coupled-cluster [23], the multiconfigurational self-consistent field [26], NEVPT2 [33], one-electron reduced density-matrix-functional theory [34], and the density-matrix renormalization-group method [35]. In this work, the CI is used. The orbitals, referred to as the HF short-range DFT orbitals in the following, are generated by restricting the minimization in the first line of Eq. (7) to single determinantal wave functions. Note that, when $\mu = 0$, the HF short-range DFT orbitals reduce to the conventional KS ones.

Finally, in connection with the description of excited states, let us mention that the exact auxiliary excited states $\{\Psi_i^{\mu}\}_{i>0}$ that fulfill the eigenvalue equation,

$$\hat{H}^{\mu}[n_{\Psi_0^{\mu}}] | \Psi_i^{\mu} \rangle = \mathcal{E}_i^{\mu} | \Psi_i^{\mu} \rangle, \quad (10)$$

can be used as starting points for reaching the physical excitation energies by means of extrapolation techniques [36–38], perturbation theory [39], TD linear response theory [4,5], or ensemble range-separated DFT [13,14], as discussed further in the following.

B. Ensemble density-functional theory for excited states

According to the GOK variational principle [6], which generalizes the seminal work of Theophilou [40] on equiensembles, the inequality

$$E^{\mathbf{w}} \leq \text{Tr}[\hat{\Gamma}^{\mathbf{w}} \hat{H}], \quad (11)$$

where $\hat{H} = \hat{T} + \hat{W}_{\text{ee}} + \hat{V}_{\text{ne}}$ and Tr denotes the trace, is fulfilled for any ensemble characterized by a set of weights $\mathbf{w} \equiv (w_0, w_1, \dots, w_{M-1})$ with $w_0 \geq w_1 \geq \dots \geq w_{M-1} > 0$ and a set of M orthonormal trial wave functions $\{\bar{\Psi}_k\}_{0 \leq k \leq M-1}$ from which a trial density matrix can be constructed:

$$\hat{\Gamma}^{\mathbf{w}} = \sum_{k=0}^{M-1} w_k |\bar{\Psi}_k\rangle \langle \bar{\Psi}_k|. \quad (12)$$

The lower bound in Eq. (11) is the exact ensemble energy

$$E^{\mathbf{w}} = \sum_{k=0}^{M-1} w_k \langle \bar{\Psi}_k | \hat{H} | \bar{\Psi}_k \rangle = \sum_{k=0}^{M-1} w_k E_k, \quad (13)$$

where Ψ_k is the exact k th eigenfunction of \hat{H} and $E_0 \leq E_1 \leq \dots \leq E_{M-1}$. In the following, the ensemble always contains complete sets of degenerate states (referred to as “multiplets” in Ref. [7]). An important consequence of the GOK principle

is that the Hohenberg-Kohn theorem can be extended to ensembles of ground and excited states [7], thus leading to the exact variational expression for the ensemble energy,

$$E^w = \min_n \left\{ F^w[n] + \int d\mathbf{r} v_{\text{ne}}(\mathbf{r})n(\mathbf{r}) \right\}, \quad (14)$$

where the universal LL ensemble functional is defined as follows:

$$F^w[n] = \min_{\hat{\Gamma}^w \rightarrow n} \{ \text{Tr}[\hat{\Gamma}^w(\hat{T} + \hat{W}_{\text{ee}})] \}. \quad (15)$$

The minimization in Eq. (15) is restricted to ensemble density matrices with the ensemble density n :

$$\text{Tr}[\hat{\Gamma}^w \hat{n}(\mathbf{r})] = n_{\hat{\Gamma}^w}(\mathbf{r}) = n(\mathbf{r}). \quad (16)$$

Note that, in the following, we use the convention $\sum_{k=0}^{M-1} w_k = 1$ so that the ensemble density integrates to the number of electrons N . The minimizing density in Eq. (14) is the exact ensemble density of the physical system $n^w(\mathbf{r}) = \sum_{k=0}^{M-1} w_k n_{\Psi_k}(\mathbf{r})$.

In standard ensemble DFT [7], which is referred to as GOK-DFT in the following, the KS partitioning of the LL functional is used,

$$F^w[n] = T_s^w[n] + E_{\text{Hxc}}^w[n], \quad (17)$$

where the noninteracting ensemble kinetic energy is defined as

$$T_s^w[n] = \min_{\hat{\Gamma}^w \rightarrow n} \{ \text{Tr}[\hat{\Gamma}^w \hat{T}] \}, \quad (18)$$

and $E_{\text{Hxc}}^w[n]$ is the \mathbf{w} -dependent Hxc functional for the ensemble, thus leading to the exact ensemble energy expression, according to Eq. (14),

$$E^w = \min_{\hat{\Gamma}^w} \{ \text{Tr}[\hat{\Gamma}^w(\hat{T} + \hat{V}_{\text{ne}})] + E_{\text{Hxc}}^w[n_{\hat{\Gamma}^w}] \}. \quad (19)$$

The minimizing GOK density matrix,

$$\hat{\Gamma}_s^w = \sum_{k=0}^{M-1} w_k |\Phi_k^w\rangle\langle\Phi_k^w|, \quad (20)$$

reproduces the exact ensemble density of the physical system,

$$n_{\hat{\Gamma}_s^w}(\mathbf{r}) = n^w(\mathbf{r}), \quad (21)$$

and it fulfills the stationarity condition $\delta\mathcal{L}^w[\hat{\Gamma}_s^w] = 0$, where

$$\begin{aligned} \mathcal{L}^w[\hat{\Gamma}^w] &= \text{Tr}[\hat{\Gamma}^w(\hat{T} + \hat{V}_{\text{ne}})] + E_{\text{Hxc}}^w[n_{\hat{\Gamma}^w}] \\ &+ \sum_{k=0}^{M-1} w_k \mathcal{E}_k^w (1 - \langle \bar{\Psi}_k | \bar{\Psi}_k \rangle). \end{aligned} \quad (22)$$

The coefficients \mathcal{E}_k^w are Lagrange multipliers associated with the normalization of the trial wave functions $\bar{\Psi}_k$ from which the density matrix is built. Considering variations $\bar{\Psi}_k \rightarrow \bar{\Psi}_k + \delta\bar{\Psi}_k$ for each individual state separately leads to the self-consistent GOK equations [7]:

$$\begin{aligned} &\left(\hat{T} + \hat{V}_{\text{ne}} + \int d\mathbf{r} \frac{\delta E_{\text{Hxc}}^w[n_{\hat{\Gamma}_s^w}]}{\delta n(\mathbf{r})} \hat{n}(\mathbf{r}) \right) |\Phi_k^w\rangle \\ &= \mathcal{E}_k^w |\Phi_k^w\rangle, \quad 0 \leq k \leq M-1. \end{aligned} \quad (23)$$

C. Range-separated ensemble density-functional theory

In analogy with ground-state range-separated DFT, the LL ensemble functional in Eq. (15) can be range-separated as [13,14]

$$F^w[n] = F^{\text{lr},\mu,w}[n] + E_{\text{Hxc}}^{\text{sr},\mu,w}[n], \quad (24)$$

where

$$F^{\text{lr},\mu,w}[n] = \min_{\hat{\Gamma}^w \rightarrow n} \{ \text{Tr}[\hat{\Gamma}^w(\hat{T} + \hat{W}_{\text{ee}}^{\text{lr},\mu})] \}. \quad (25)$$

In the following, the short-range ensemble functional is partitioned into \mathbf{w} -independent Hartree and \mathbf{w} -dependent xc terms,

$$E_{\text{Hxc}}^{\text{sr},\mu,w}[n] = E_{\text{H}}^{\text{sr},\mu}[n] + E_{\text{xc}}^{\text{sr},\mu,w}[n]. \quad (26)$$

Note that the decomposition is arbitrary and can be exact or not, depending on the short-range xc functional used. In practical calculations, local and semilocal xc functionals may not remove the so-called ‘‘ghost interactions’’ [41,42] that are included in the short-range Hartree term. Such interactions are fictitious and unwanted. Their detailed analysis, in the context of range-separated ensemble DFT, is currently in progress and will be presented in a separate work.

Combining Eq. (14) with Eq. (24) leads to the exact range-separated ensemble energy expression

$$E^w = \min_{\hat{\Gamma}^w} \{ \text{Tr}[\hat{\Gamma}^w(\hat{T} + \hat{W}_{\text{ee}}^{\text{lr},\mu} + \hat{V}_{\text{ne}})] + E_{\text{Hxc}}^{\text{sr},\mu,w}[n_{\hat{\Gamma}^w}] \}. \quad (27)$$

The minimizing long-range-interacting ensemble density matrix $\hat{\Gamma}^{\mu,w} = \sum_{k=0}^{M-1} w_k |\Psi_k^{\mu,w}\rangle\langle\Psi_k^{\mu,w}|$ reproduces the physical ensemble density,

$$n_{\hat{\Gamma}^{\mu,w}}(\mathbf{r}) = n^w(\mathbf{r}), \quad (28)$$

and by analogy with Eq. (22), we conclude that it should fulfill the self-consistent equation

$$\begin{aligned} &\left(\hat{T} + \hat{W}_{\text{ee}}^{\text{lr},\mu} + \hat{V}_{\text{ne}} + \int d\mathbf{r} \frac{\delta E_{\text{Hxc}}^{\text{sr},\mu,w}[n_{\hat{\Gamma}^{\mu,w}}]}{\delta n(\mathbf{r})} \hat{n}(\mathbf{r}) \right) |\Psi_k^{\mu,w}\rangle \\ &= \mathcal{E}_k^{\mu,w} |\Psi_k^{\mu,w}\rangle, \quad 0 \leq k \leq M-1. \end{aligned} \quad (29)$$

Note that the Schrödinger and GOK-DFT equations are recovered for $\mu \rightarrow +\infty$ and $\mu = 0$, respectively.

In the rest of this work we mainly focus on ensembles consisting of two nondegenerate states. In this case, the ensemble weights are simply equal to

$$w_1 = w, \quad w_0 = 1 - w, \quad (30)$$

where $0 \leq w \leq 1/2$, and the exact ensemble energy is a linear function of w ,

$$E^w = (1 - w)E_0 + w E_1. \quad (31)$$

Consequently, the first excitation energy $\omega = E_1 - E_0$ can be written either as a first-order derivative,

$$\omega = \frac{dE^w}{dw}, \quad (32)$$

or as the slope of the linear interpolation between $w = 0$ and $w = 1/2$,

$$\omega = 2(E^{w=1/2} - E_0). \quad (33)$$

Let us stress that Eqs. (32) and (33) are equivalent in the exact theory. By using the decomposition [see Eqs. (27) and (28)]

$$E^w = (1-w)\langle \Psi_0^{\mu,w} | \hat{T} + \hat{W}_{\text{ee}}^{\text{lr},\mu} + \hat{V}_{\text{ne}} | \Psi_0^{\mu,w} \rangle + w\langle \Psi_1^{\mu,w} | \hat{T} + \hat{W}_{\text{ee}}^{\text{lr},\mu} + \hat{V}_{\text{ne}} | \Psi_1^{\mu,w} \rangle + E_{\text{Hxc}}^{\text{sr},\mu,w}[n^w], \quad (34)$$

which can be rewritten in terms of the auxiliary long-range interacting energies, according to Eq. (29), as

$$E^w = (1-w)\mathcal{E}_0^{\mu,w} + w\mathcal{E}_1^{\mu,w} - \int d\mathbf{r} \frac{\delta E_{\text{Hxc}}^{\text{sr},\mu,w}[n^w]}{\delta n(\mathbf{r})} n^w(\mathbf{r}) + E_{\text{Hxc}}^{\text{sr},\mu,w}[n^w], \quad (35)$$

where the physical ensemble density equals the auxiliary one [see Eq. (28)],

$$n^w(\mathbf{r}) = (1-w)n_{\Psi_0^{\mu,w}}(\mathbf{r}) + wn_{\Psi_1^{\mu,w}}(\mathbf{r}), \quad (36)$$

and by applying the Hellmann-Feynman theorem,

$$\frac{d\mathcal{E}_i^{\mu,w}}{dw} = \int d\mathbf{r} \frac{\partial}{\partial w} \left(\frac{\delta E_{\text{Hxc}}^{\text{sr},\mu,w}[n^w]}{\delta n(\mathbf{r})} \right) n_{\Psi_i^{\mu,w}}(\mathbf{r}), \quad (37)$$

we finally recover from Eq. (32) the following expression for the first excitation energy [14]:

$$\begin{aligned} \omega &= \mathcal{E}_1^{\mu,w} - \mathcal{E}_0^{\mu,w} + \left. \frac{\partial E_{\text{Hxc}}^{\text{sr},\mu,w}[n]}{\partial w} \right|_{n=n^w} \\ &= \Delta\mathcal{E}^{\mu,w} + \Delta_{\text{xc}}^{\mu,w}. \end{aligned} \quad (38)$$

It is readily seen from Eq. (38) that the auxiliary excitation energy $\Delta\mathcal{E}^{\mu,w} = \mathcal{E}_1^{\mu,w} - \mathcal{E}_0^{\mu,w}$ differs in principle from the physical one. They become equal when $\mu \rightarrow +\infty$. For finite μ values, the difference is simply expressed in terms of a derivative with respect to the ensemble weight $\Delta_{\text{xc}}^{\mu,w} = \partial E_{\text{Hxc}}^{\text{sr},\mu,w}[n]/\partial w|_{n=n^w}$. Note that the Hartree term does not contribute to the second term on the right-hand side of Eq. (38) since it is, for a given density n , w independent [see Eq. (26)]. Interestingly, when $w \rightarrow 0$, an exact expression for the physical excitation energy is obtained in terms of the auxiliary one, which is associated with the ground-state density [see Eq. (10)],

$$\omega = \mathcal{E}_1^\mu - \mathcal{E}_0^\mu + \left. \frac{\partial E_{\text{Hxc}}^{\text{sr},\mu,w}[n^0]}{\partial w} \right|_{w=0}. \quad (39)$$

Note also that, when $\mu = 0$ and the first excitation is a one-particle-one-hole excitation (single excitation), the GOK expression [7] is recovered from Eq. (38),

$$\omega = \Delta\epsilon^w + \Delta_{\text{xc}}^w, \quad (40)$$

where $\Delta\epsilon^w = \varepsilon_1^w - \varepsilon_0^w$ is the HOMO-LUMO gap for the noninteracting ensemble and $\Delta_{\text{xc}}^w = \partial E_{\text{Hxc}}^w[n]/\partial w|_{n=n^w}$. In the $w \rightarrow 0$ limit, the exact excitation energy can be expressed in terms of the KS HOMO ε_0 and LUMO ε_1 energies as

$$\omega = \varepsilon_1^{w \rightarrow 0} - \varepsilon_0, \quad (41)$$

where $\varepsilon_1^{w \rightarrow 0} = \varepsilon_1 + \Delta_{\text{xc}}^0$. As shown analytically by Levy [43] and numerically by Yang *et al.* [15], Δ_{xc}^0 corresponds to the jump in the xc potential when moving from $w = 0$ (ground state) to $w > 0$ (ensemble of ground and excited states). This is known as the derivative discontinuity (DD) and should not

be confused with the ground-state DD, which is related to ionization energies and electron affinities, although there are distinct similarities at a formal level [44–46]. Consequently, the quantity $\Delta_{\text{xc}}^{\mu,w}$ introduced in Eq. (38) is referred to in the following as short-range DD.

D. Weight-independent density-functional approximation and the linear interpolation method

Even though an exact adiabatic-connection-based expression exists for the short-range ensemble xc functional (see Eq. (133) in Ref. [14]), it has not been used yet for developing weight-dependent density-functional approximations. Let us stress that this is still a challenge also in the context of GOK-DFT [15]. A crude approximation simply consists in using the ground-state functional [13],

$$E_{\text{xc}}^{\text{sr},\mu,w}[n] \rightarrow E_{\text{xc}}^{\text{sr},\mu}[n], \quad (42)$$

thus leading to the approximate ensemble energy expression

$$\begin{aligned} \tilde{E}^{\mu,w} &= (1-w)\langle \tilde{\Psi}_0^{\mu,w} | \hat{T} + \hat{W}_{\text{ee}}^{\text{lr},\mu} + \hat{V}_{\text{ne}} | \tilde{\Psi}_0^{\mu,w} \rangle \\ &+ w\langle \tilde{\Psi}_1^{\mu,w} | \hat{T} + \hat{W}_{\text{ee}}^{\text{lr},\mu} + \hat{V}_{\text{ne}} | \tilde{\Psi}_1^{\mu,w} \rangle + E_{\text{Hxc}}^{\text{sr},\mu}[\tilde{n}^{\mu,w}], \end{aligned} \quad (43)$$

which may depend on both μ and w , and where the approximate auxiliary ensemble density equals

$$\tilde{n}^{\mu,w}(\mathbf{r}) = (1-w)n_{\tilde{\Psi}_0^{\mu,w}}(\mathbf{r}) + wn_{\tilde{\Psi}_1^{\mu,w}}(\mathbf{r}), \quad (44)$$

with

$$\hat{H}^\mu[\tilde{n}^{\mu,w}]|\tilde{\Psi}_i^{\mu,w}\rangle = \tilde{\mathcal{E}}_i^{\mu,w}|\tilde{\Psi}_i^{\mu,w}\rangle, \quad i = 0,1. \quad (45)$$

In the following we refer to this approximation as the WIDFA. Note that, at the WIDFA level, the ground-state density-functional Hamiltonian $\hat{H}^\mu[n]$ [see Eq. (9)] is used. The auxiliary wave functions $\tilde{\Psi}_i^{\mu,w}$ associated with the biensemble ($0 < w \leq 1/2$) will therefore deviate from their “ground-state” limits Ψ_i^μ ($w = 0$) because of the ensemble density $\tilde{n}^{\mu,w}$, which is inserted into the short-range Hxc potential. Note that Eq. (45) should be solved self-consistently. Let us also stress that the ground-state short-range Hxc density-functional potential $\delta E_{\text{Hxc}}^{\text{sr},\mu}[n^0]/\delta n(\mathbf{r})$ is recovered in the limit $w \rightarrow 0$, as readily seen from Eq. (45). In other words, the short-range DD is not modeled at the WIDFA level of approximation. Finally, the exact (μ -independent) ground-state energy will still be recovered when $w \rightarrow 0$ if no approximation is introduced in the short-range xc functional,

$$\tilde{E}^{\mu,0} = E_0. \quad (46)$$

Obviously, the exact ensemble energy will in general not be recovered for $w > 0$. By rewriting the WIDFA ensemble energy as

$$\begin{aligned} \tilde{E}^{\mu,w} &= (1-w)\tilde{\mathcal{E}}_0^{\mu,w} + w\tilde{\mathcal{E}}_1^{\mu,w} \\ &- \int d\mathbf{r} \frac{\delta E_{\text{Hxc}}^{\text{sr},\mu}[\tilde{n}^{\mu,w}]}{\delta n(\mathbf{r})} \tilde{n}^{\mu,w}(\mathbf{r}) + E_{\text{Hxc}}^{\text{sr},\mu}[\tilde{n}^{\mu,w}] \end{aligned} \quad (47)$$

and applying the Hellmann-Feynman theorem,

$$\frac{d\tilde{\mathcal{E}}_i^{\mu,w}}{dw} = \int d\mathbf{r} \frac{\partial}{\partial w} \left(\frac{\delta E_{\text{Hxc}}^{\text{sr},\mu}[\tilde{n}^{\mu,w}]}{\delta n(\mathbf{r})} \right) n_{\tilde{\Psi}_i^{\mu,w}}(\mathbf{r}), \quad (48)$$

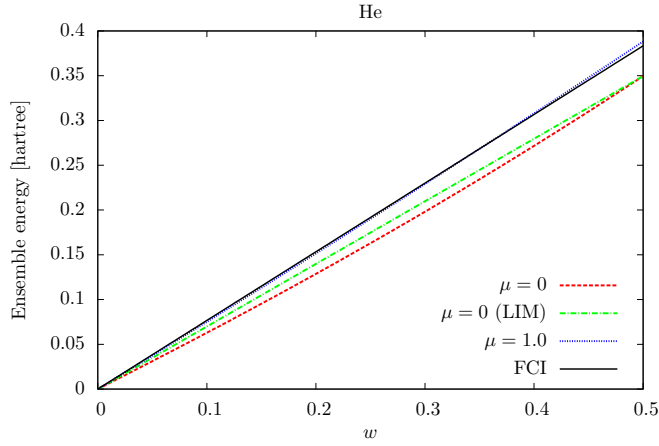


FIG. 1. (Color online) Range-separated ensemble energy obtained for He at the WIDFA level while varying the ensemble weight w for $\mu = 0$ and $1.0a_0^{-1}$. Comparison is made with the linear interpolation method (LIM) for $\mu = 0a_0^{-1}$ and full configuration interaction (FCI). The ensemble contains both 1^1S and 2^1S states. The srLDA functional was used.

we see that, within the WIDFA, the first-order derivative of the ensemble energy reduces to the auxiliary excitation energy, which is, in principle, w dependent,

$$\frac{d\tilde{E}^{\mu,w}}{dw} = \tilde{\mathcal{E}}_1^{\mu,w} - \tilde{\mathcal{E}}_0^{\mu,w} = \Delta\tilde{\mathcal{E}}^{\mu,w}. \quad (49)$$

Therefore, in practical calculations, the WIDFA ensemble energy may not be strictly linear in w , as illustrated for He in Fig. 1. In the same spirit as Ref. [17], we propose to restore the linearity by means of a simple linear interpolation between the ground state ($w = 0$) and the equiensemble ($w = 1/2$),

$$\bar{E}^{\mu,w} = E_0 + 2w(\tilde{E}^{\mu,1/2} - E_0). \quad (50)$$

This approach, which is rationalized in Sec. II E, is referred to as the LIM in the following. The approximate excitation energy is then unambiguously defined as

$$\omega_{\text{LIM}}^{\mu} = \frac{d\bar{E}^{\mu,w}}{dw} = 2(\tilde{E}^{\mu,1/2} - E_0). \quad (51)$$

Note that, according to Eq. (33), the LIM becomes exact when the exact weight-dependent short-range xc functional is used. By analogy with the grand canonical ensemble [17], we can connect the linear interpolated and curved WIDFA ensemble energies as

$$\bar{E}^{\mu,w} = \tilde{E}^{\mu,w} + \int_0^w d\xi \Delta_{\text{eff}}^{\mu,\xi}, \quad (52)$$

so that, according to Eqs. (49) and (51),

$$\omega_{\text{LIM}}^{\mu} = \Delta\tilde{\mathcal{E}}^{\mu,w} + \Delta_{\text{eff}}^{\mu,w}. \quad (53)$$

As readily seen from Eqs. (38) and (53), $\Delta_{\text{eff}}^{\mu,w}$ plays the role of an effective DD that corrects for the curvature of the WIDFA ensemble energy, thus ensuring strict linearity in w . A graphical representation of LIM is shown in Fig. 2.

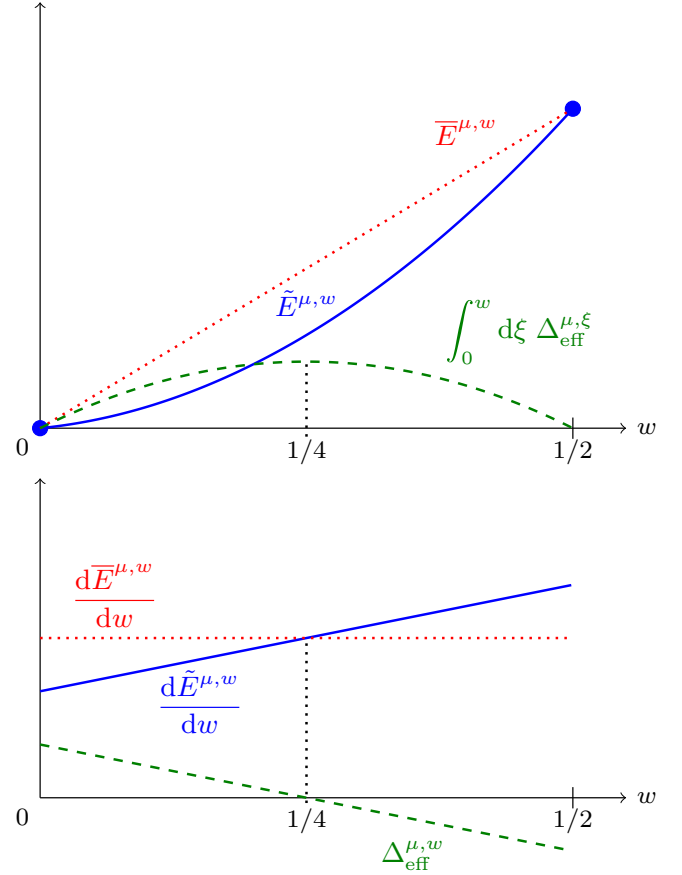


FIG. 2. (Color online) Schematic of the linear interpolation method. Top: Ensemble energies. Bottom: Their first-order derivatives. See text for further details.

E. Rationale for LIM and the effective DD

The effective DD has been introduced in Eq. (52) for the purpose of recovering an approximate range-separated ensemble energy that is strictly linear in w . This choice can be rationalized when using a range-dependent generalized adiabatic connection formalism for ensembles [14], where the exact short-range ensemble potential is adjusted so that the auxiliary ensemble density equals the (weight-independent) density $n(\mathbf{r})$ for any weight ξ and range-separation parameter ν values,

$$\left(\hat{T} + \hat{W}_{\text{ee}}^{\text{lr},\nu} + \int d\mathbf{r} v^{\nu,\xi}(\mathbf{r}) \hat{n}(\mathbf{r}) \right) |\Psi_i^{\nu,\xi}\rangle = \mathcal{E}_i^{\nu,\xi} |\Psi_i^{\nu,\xi}\rangle, \quad (54)$$

$$i = 0, 1,$$

where

$$(1 - \xi)n_{\Psi_0^{\nu,\xi}}(\mathbf{r}) + \xi n_{\Psi_1^{\nu,\xi}}(\mathbf{r}) = n(\mathbf{r}). \quad (55)$$

It was shown [14] that the exact short-range ensemble xc density-functional energy can be formally connected with its ground-state limit ($w = 0$) as

$$E_{\text{xc}}^{\text{sr},\mu,w}[n] = E_{\text{xc}}^{\text{sr},\mu}[n] + \int_0^w d\xi \Delta_{\text{xc}}^{\text{sr},\mu,\xi}[n], \quad (56)$$

where the exact density-functional DD equals

$$\Delta_{\text{xc}}^{\text{sr},\mu,\xi}[n] = (\mathcal{E}_1^{+\infty,\xi} - \mathcal{E}_0^{+\infty,\xi}) - (\mathcal{E}_1^{\mu,\xi} - \mathcal{E}_0^{\mu,\xi}). \quad (57)$$

When rewriting the WIDFA ensemble energy in Eq. (43) as

$$\begin{aligned} \tilde{E}^{\mu,w} &= F^{\text{lr},\mu,w}[\tilde{n}^{\mu,w}] + E_{\text{Hxc}}^{\text{sr},\mu}[\tilde{n}^{\mu,w}] \\ &+ \int d\mathbf{r} v_{\text{nc}}(\mathbf{r})\tilde{n}^{\mu,w}(\mathbf{r}), \end{aligned} \quad (58)$$

it becomes clear, from Eqs. (52) and (56), that the LIM implicitly defines an approximate weight-dependent short-range xc functional:

$$E_{\text{xc}}^{\text{sr},\mu,w}[\tilde{n}^{\mu,w}] \rightarrow E_{\text{xc}}^{\text{sr},\mu}[\tilde{n}^{\mu,w}] + \int_0^w d\xi \Delta_{\text{eff}}^{\mu,\xi}. \quad (59)$$

In order to connect the exact DD with the effective one, let us consider Eq. (57) in the particular case $n = \tilde{n}^{\mu,w}$ and $\xi = w$, thus leading to

$$\Delta_{\text{xc}}^{\text{sr},\mu,w}[\tilde{n}^{\mu,w}] = \Delta\tilde{\mathcal{E}}^{+\infty,w} - \Delta\tilde{\mathcal{E}}^{\mu,w}, \quad (60)$$

where $\Delta\tilde{\mathcal{E}}^{+\infty,w}$ is the excitation energy of the fully interacting system with ensemble density $\tilde{n}^{\mu,w}$. If the latter is a good approximation to the true physical ensemble density n^w , which is the basic assumption in the WIDFA, then $\Delta\tilde{\mathcal{E}}^{+\infty,w}$ becomes w independent and equals the true physical excitation energy. As discussed previously, the latter has various approximate expressions that all rely on various exact expressions. Choosing the slope of the linearly interpolated WIDFA ensemble energy $\omega_{\text{LIM}}^{\mu}$ is, in principle, as relevant as other choices. Still, the analytical derivations and numerical results presented in the following suggest that the LIM has many advantages from a practical point of view. By doing so, we finally recover the expression in Eq. (53):

$$\Delta_{\text{xc}}^{\text{sr},\mu,w}[\tilde{n}^{\mu,w}] \rightarrow \omega_{\text{LIM}}^{\mu} - \Delta\tilde{\mathcal{E}}^{\mu,w}. \quad (61)$$

F. Effective DD and excitation energy for a quadratic range-separated ensemble energy

For analysis purposes we approximate the WIDFA ensemble energy by its Taylor expansion through second order in w (around $w = 0$) over the interval $[0, 1/2]$,

$$\tilde{E}^{\mu,w} \rightarrow \check{E}^{\mu,w} = E_0 + w\tilde{E}^{\mu(1)} + \frac{w^2}{2}\tilde{E}^{\mu(2)}, \quad (62)$$

where, according to Eqs. (10), (45), (48), and (49),

$$\tilde{E}^{\mu(1)} = \left. \frac{d\tilde{E}^{\mu,w}}{dw} \right|_{w=0} = \mathcal{E}_1^{\mu} - \mathcal{E}_0^{\mu} \quad (63)$$

and

$$\begin{aligned} \tilde{E}^{\mu(2)} &= \left. \frac{d^2\tilde{E}^{\mu,w}}{dw^2} \right|_{w=0} \\ &= \iint d\mathbf{r}d\mathbf{r}' \frac{\delta^2 E_{\text{Hxc}}^{\text{sr},\mu}[n^0]}{\delta n(\mathbf{r}')\delta n(\mathbf{r})} (n_{\Psi_1^{\mu}}(\mathbf{r}) - n^0(\mathbf{r})) \\ &\quad \times \left(n_{\Psi_1^{\mu}}(\mathbf{r}') - n^0(\mathbf{r}') + \left. \frac{\partial n_{\Psi_0^{\mu,w}}(\mathbf{r}')}{\partial w} \right|_{w=0} \right). \end{aligned} \quad (64)$$

As shown in Sec. IV, this approximation is accurate when $\mu \geq 1.0a_0^{-1}$. For smaller μ values, and especially in the GOK-DFT limit ($\mu = 0$), the WIDFA ensemble energy is usually not

quadratic in w . Nevertheless, making such an approximation gives further insight into the LIM approach, as shown in the following. From the equiensemble energy expression

$$\check{E}^{\mu,1/2} = E_0 + \frac{1}{2}\tilde{E}^{\mu(1)} + \frac{1}{8}\tilde{E}^{\mu(2)} \quad (65)$$

and Eq. (51), we obtain the LIM excitation energy within the quadratic approximation, which we refer to as the LIM2,

$$\omega_{\text{LIM2}}^{\mu} = 2(\check{E}^{\mu,1/2} - E_0) = \tilde{E}^{\mu(1)} + \frac{1}{4}\tilde{E}^{\mu(2)}, \quad (66)$$

thus leading to

$$\begin{aligned} \omega_{\text{LIM2}}^{\mu} &= \mathcal{E}_1^{\mu} - \mathcal{E}_0^{\mu} \\ &+ \frac{1}{4} \iint d\mathbf{r}d\mathbf{r}' \frac{\delta^2 E_{\text{Hxc}}^{\text{sr},\mu}[n^0]}{\delta n(\mathbf{r}')\delta n(\mathbf{r})} (n_{\Psi_1^{\mu}}(\mathbf{r}) - n^0(\mathbf{r})) \\ &\quad \times \left(n_{\Psi_1^{\mu}}(\mathbf{r}') - n^0(\mathbf{r}') + \left. \frac{\partial n_{\Psi_0^{\mu,w}}(\mathbf{r}')}{\partial w} \right|_{w=0} \right). \end{aligned} \quad (67)$$

As shown in Appendix A, an explicit expression for the linear response of the ground-state density $n_{\Psi_0^{\mu,w}}$ to variations in the ensemble weight w can be obtained from self-consistent perturbation theory. Thus we obtain the following expansion through second order in the short-range kernel:

$$\begin{aligned} \omega_{\text{LIM2}}^{\mu} &= \mathcal{E}_1^{\mu} - \mathcal{E}_0^{\mu} \\ &+ \frac{1}{4} \iint d\mathbf{r}d\mathbf{r}' \frac{\delta^2 E_{\text{Hxc}}^{\text{sr},\mu}[n^0]}{\delta n(\mathbf{r}')\delta n(\mathbf{r})} (n_{\Psi_1^{\mu}}(\mathbf{r}') - n^0(\mathbf{r}')) \\ &\quad \times (n_{\Psi_1^{\mu}}(\mathbf{r}) - n^0(\mathbf{r})) \\ &+ \frac{1}{2} \iiint d\mathbf{r}_1 d\mathbf{r}'_1 d\mathbf{r}d\mathbf{r}' \frac{\delta^2 E_{\text{Hxc}}^{\text{sr},\mu}[n^0]}{\delta n(\mathbf{r}'_1)\delta n(\mathbf{r})} \\ &\quad \times \frac{\delta^2 E_{\text{Hxc}}^{\text{sr},\mu}[n^0]}{\delta n(\mathbf{r}')\delta n(\mathbf{r})} (n_{\Psi_1^{\mu}}(\mathbf{r}) - n^0(\mathbf{r})) \\ &\quad \times (n_{\Psi_1^{\mu}}(\mathbf{r}'_1) - n^0(\mathbf{r}'_1)) \sum_{i \geq 1} \frac{n_{0i}^{\mu}(\mathbf{r}_1)n_{0i}^{\mu}(\mathbf{r}')}{\mathcal{E}_0^{\mu} - \mathcal{E}_i^{\mu}} + \dots \end{aligned} \quad (68)$$

The latter expression is convenient for comparing the LIM with TD range-separated DFT, as discussed further in the following. Returning to the quadratic ensemble energy in Eq. (62), its first-order derivative equals

$$\frac{d\check{E}^{\mu,w}}{dw} = \tilde{E}^{\mu(1)} + w\tilde{E}^{\mu(2)}, \quad (69)$$

thus leading to the following expression for the effective DD, according to Eq. (66):

$$\check{\Delta}_{\text{eff}}^{\mu,w} = \omega_{\text{LIM2}}^{\mu} - \frac{d\check{E}^{\mu,w}}{dw} = \left(\frac{1}{4} - w \right) \tilde{E}^{\mu(2)}. \quad (70)$$

In conclusion, the effective DD is expected to vanish at $w = 1/4$ when the WIDFA ensemble energy is strictly quadratic, as illustrated in Fig. 2.

G. Comparison with existing methods

1. Excitation energies from individual densities

Pastorzak *et al.* [13] recently proposed computing excitation energies as individual total energy differences,

$$\Delta E(w) = E_1(w) - E_0(w), \quad (71)$$

where the energy associated with state i ($i = 0, 1$) is obtained from its (individual) density as follows:

$$E_i(w) = \langle \tilde{\Psi}_i^{\mu,w} | \hat{T} + \hat{W}_{\text{ec}}^{\text{lr},\mu} + \hat{V}_{\text{nc}} | \tilde{\Psi}_i^{\mu,w} \rangle + E_{\text{Hxc}}^{\text{sr},\mu} [n_{\tilde{\Psi}_i^{\mu,w}}]. \quad (72)$$

From the Taylor expansion

$$\Delta E(w) = \Delta E(0) + w \left. \frac{d\Delta E(w)}{dw} \right|_{w=0} + O(w^2), \quad (73)$$

where

$$\begin{aligned} \Delta E(0) &= \mathcal{E}_1^\mu - \mathcal{E}_0^\mu + E_{\text{Hxc}}^{\text{sr},\mu} [n_{\Psi_1^\mu}] - E_{\text{Hxc}}^{\text{sr},\mu} [n^0] \\ &+ \int d\mathbf{r} \frac{\delta E_{\text{Hxc}}^{\text{sr},\mu} [n^0]}{\delta n(\mathbf{r})} (n^0(\mathbf{r}) - n_{\Psi_1^\mu}(\mathbf{r})), \end{aligned} \quad (74)$$

and according to Eq. (48),

$$\begin{aligned} \left. \frac{d\Delta E(w)}{dw} \right|_{w=0} &= \int d\mathbf{r} \left(\frac{\delta E_{\text{Hxc}}^{\text{sr},\mu} [n_{\Psi_1^\mu}]}{\delta n(\mathbf{r})} - \frac{\delta E_{\text{Hxc}}^{\text{sr},\mu} [n^0]}{\delta n(\mathbf{r})} \right) \\ &\times \left. \frac{\partial n_{\tilde{\Psi}_1^{\mu,w}}(\mathbf{r})}{\partial w} \right|_{w=0}, \end{aligned} \quad (75)$$

it is readily seen that the excitation energy will vary linearly with w in the vicinity of $w = 0$. Therefore, in practical calculations, an optimal value for w must be determined [13]. This scheme can be compared with the LIM2 by expanding the excitation energy in the density difference $n_{\Psi_1^\mu}(\mathbf{r}) - n^0(\mathbf{r})$, thus leading to

$$\begin{aligned} \Delta E(w) &= \mathcal{E}_1^\mu - \mathcal{E}_0^\mu \\ &+ \frac{1}{2} \iint d\mathbf{r} d\mathbf{r}' \frac{\delta^2 E_{\text{Hxc}}^{\text{sr},\mu} [n^0]}{\delta n(\mathbf{r}') \delta n(\mathbf{r})} (n_{\Psi_1^\mu}(\mathbf{r}') - n^0(\mathbf{r}')) \\ &\times (n_{\Psi_1^\mu}(\mathbf{r}) - n^0(\mathbf{r})) \\ &+ w \iint d\mathbf{r} d\mathbf{r}' \frac{\delta^2 E_{\text{Hxc}}^{\text{sr},\mu} [n^0]}{\delta n(\mathbf{r}') \delta n(\mathbf{r})} (n_{\Psi_1^\mu}(\mathbf{r}') - n^0(\mathbf{r}')) \\ &\times \left. \frac{\partial n_{\tilde{\Psi}_1^{\mu,\xi}}(\mathbf{r})}{\partial \xi} \right|_{\xi=0} + \dots \end{aligned} \quad (76)$$

or, equivalently,

$$\begin{aligned} \Delta E(w) &= \mathcal{E}_1^\mu - \mathcal{E}_0^\mu \\ &+ \frac{1}{4} \iint d\mathbf{r} d\mathbf{r}' \frac{\delta^2 E_{\text{Hxc}}^{\text{sr},\mu} [n^0]}{\delta n(\mathbf{r}') \delta n(\mathbf{r})} (n_{\Psi_1^\mu}(\mathbf{r}') - n^0(\mathbf{r}')) \\ &\times \left(n_{\Psi_1^\mu}(\mathbf{r}) - n^0(\mathbf{r}) + \left. \frac{\partial \tilde{n}^{\mu,w,\xi}(\mathbf{r})}{\partial \xi} \right|_{\xi=0} \right) + \dots, \end{aligned} \quad (77)$$

where

$$\tilde{n}^{\mu,w,\xi}(\mathbf{r}) = (4w + \xi) n_{\tilde{\Psi}_1^{\mu,\xi}}(\mathbf{r}) - \xi n_{\tilde{\Psi}_0^{\mu,\xi}}(\mathbf{r}). \quad (78)$$

This expression is recovered from the LIM2 excitation energy in Eq. (67) by applying the following substitution:

$$n_{\tilde{\Psi}_0^{\mu,\xi}}(\mathbf{r}) \rightarrow \tilde{n}^{\mu,w,\xi}(\mathbf{r}). \quad (79)$$

In other words, for a given ensemble weight w , the response of $\tilde{n}^{\mu,w,\xi}$ is used rather than the ground-state density response in the calculation of the excitation energy $\Delta E(w)$. Note that integrating $\tilde{n}^{\mu,w,\xi}$ over space gives $4wN$. Therefore, $\tilde{n}^{\mu,w,\xi}$ may be considered as a density only when $w = 1/4$. In this case, it is simply expressed as

$$\tilde{n}^{\mu,1/4,\xi}(\mathbf{r}) = (1 + \xi) n_{\tilde{\Psi}_1^{\mu,\xi}}(\mathbf{r}) - \xi n_{\tilde{\Psi}_0^{\mu,\xi}}(\mathbf{r}), \quad (80)$$

and its response to changes in ξ equals

$$\left. \frac{\partial \tilde{n}^{\mu,1/4,\xi}(\mathbf{r})}{\partial \xi} \right|_{\xi=0} = n_{\Psi_1^\mu}(\mathbf{r}) - n^0(\mathbf{r}) + \left. \frac{\partial n_{\tilde{\Psi}_1^{\mu,\xi}}(\mathbf{r})}{\partial \xi} \right|_{\xi=0}. \quad (81)$$

Consequently, the LIM2 excitation energy can be recovered only if $n_{\tilde{\Psi}_0^{\mu,\xi}} = n_{\tilde{\Psi}_1^{\mu,\xi}}$ around $\xi = 0$, which means that the excitation energy equals the auxiliary one. Note, finally, that the averaged density in Eq. (80) can be interpreted as an ensemble density only if $-1 \leq \xi \leq -1/2$. It is unclear whether its derivative at $\xi = 0$ has any physical meaning.

2. Time-dependent adiabatic linear response theory

An approximation $\tilde{\omega}$ to the first excitation energy can also be determined from range-separated DFT within the adiabatic TD linear response regime [4,5]. The associated linear response vector X fulfills

$$(E_0^{[2]\mu} + K_{\text{Hxc}}^{\text{sr},\mu} - \tilde{\omega} S^{[2]\mu}) X = 0, \quad (82)$$

where the long-range interacting Hessian and the metric equal

$$E_0^{[2]\mu} = \begin{bmatrix} [\hat{R}_i, [\hat{H}_0^\mu, \hat{R}_j^\dagger]]_0 & [\hat{R}_i, [\hat{H}_0^\mu, \hat{R}_j]]_0 \\ ([\hat{R}_i, [\hat{H}_0^\mu, \hat{R}_j]]_0)^* & ([\hat{R}_i, [\hat{H}_0^\mu, \hat{R}_j^\dagger]]_0)^* \end{bmatrix} \quad (83)$$

and

$$S^{[2]\mu} = \begin{bmatrix} [\hat{R}_i, \hat{R}_j^\dagger]_0 & [\hat{R}_i, \hat{R}_j]_0 \\ -([\hat{R}_i, \hat{R}_j]_0)^* & -([\hat{R}_i, \hat{R}_j^\dagger]_0)^* \end{bmatrix}, \quad (84)$$

respectively. Shorthand notations $[\hat{A}, \hat{B}]_0 = \langle \Psi_0^\mu | [\hat{A}, \hat{B}] | \Psi_0^\mu \rangle$, $\hat{H}_0^\mu = \hat{H}^\mu [n^0]$, and $R_i^\dagger = |\Psi_i^\mu\rangle \langle \Psi_0^\mu|$ with $i > 0$ have been used. The short-range kernel matrix in Eq. (82) is written as

$$K_{\text{Hxc}}^{\text{sr},\mu} = \iint d\mathbf{r} d\mathbf{r}' \frac{\delta^2 E_{\text{Hxc}}^{\text{sr},\mu} [n^0]}{\delta n(\mathbf{r}') \delta n(\mathbf{r})} n^{[1]\mu}(\mathbf{r}') n^{[1]\mu\dagger}(\mathbf{r}), \quad (85)$$

where the gradient density vector equals

$$n^{[1]\mu}(\mathbf{r}) = \begin{bmatrix} [\hat{R}_i, \hat{n}(\mathbf{r})]_0 \\ [\hat{R}_i^\dagger, \hat{n}(\mathbf{r})]_0 \end{bmatrix}. \quad (86)$$

Since we use in this section a complete basis of orthonormal N -electron eigenfunctions $\{\Psi_k^\mu\}_{k=0,1,\dots}$ associated with the unperturbed long-range interacting Hamiltonian $\hat{H}^\mu [n^0]$ and the energies $\{\mathcal{E}_k^\mu\}_{k=0,1,\dots}$, orbital rotations do not need to be considered, in contrast to the approximate multideterminant formulations presented in Refs. [4,5], such that the matrices

simply reduce to

$$E_0^{[2]\mu} = \begin{bmatrix} (\mathcal{E}_i^\mu - \mathcal{E}_0^\mu)\delta_{ij} & 0 \\ 0 & (\mathcal{E}_i^\mu - \mathcal{E}_0^\mu)\delta_{ij} \end{bmatrix}, \quad (87)$$

$$S^{[2]\mu} = \begin{bmatrix} \delta_{ij} & 0 \\ 0 & -\delta_{ij} \end{bmatrix},$$

and the gradient density vector becomes

$$n^{[1]\mu}(\mathbf{r}) = \begin{bmatrix} n_{0i}^\mu(\mathbf{r}) \\ -n_{0i}^\mu(\mathbf{r}) \end{bmatrix}. \quad (88)$$

The transition matrix elements associated with the density operator $n_{0i}^\mu(\mathbf{r})$ have been introduced in Eq. (A8).

We propose to solve Eq. (82) by means of perturbation theory in order to make a comparison with the LIM2. The perturbation will be the short-range kernel. Let us consider the auxiliary linear response equation,

$$(E_0^{[2]\mu} + \alpha K_{\text{Hxc}}^{\text{sr},\mu} - \omega(\alpha)S^{[2]\mu})X(\alpha) = 0, \quad (89)$$

which reduces to Eq. (82) in the $\alpha = 1$ limit, and the perturbation expansions

$$X(\alpha) = X^{(0)} + \alpha X^{(1)} + O(\alpha^2), \quad (90)$$

$$\omega(\alpha) = \omega^{(0)} + \alpha\omega^{(1)} + \alpha^2\omega^{(2)} + O(\alpha^3).$$

Since we are interested here in the first excitation energy only, we have

$$X^{(0)} = \begin{bmatrix} 1 \\ 0 \\ \vdots \\ 0 \end{bmatrix}, \quad \omega^{(0)} = \mathcal{E}_1^\mu - \mathcal{E}_0^\mu. \quad (91)$$

Inserting Eq. (90) into Eq. (89) leads to the following excitation energy corrections through second order,

$$\omega^{(1)} = X^{(0)\dagger} K_{\text{Hxc}}^{\text{sr},\mu} X^{(0)}, \quad (92)$$

$$\omega^{(2)} = X^{(0)\dagger} K_{\text{Hxc}}^{\text{sr},\mu} X^{(1)},$$

where the intermediate normalization condition $X(\alpha)^\dagger S^{[2]\mu} X^{(0)} = 1$ has been used, and

$$(E_0^{[2]\mu} - \omega^{(0)}S^{[2]\mu})X^{(1)} = -K_{\text{Hxc}}^{\text{sr},\mu} X^{(0)} + \omega^{(1)}S^{[2]\mu} X^{(0)}. \quad (93)$$

According to Eqs. (85), (88), and (91), the first-order corrections to the excitation energy and the linear response vector become

$$\omega^{(1)} = \iint d\mathbf{r}d\mathbf{r}' \frac{\delta^2 E_{\text{Hxc}}^{\text{sr},\mu}[n^0]}{\delta n(\mathbf{r}')\delta n(\mathbf{r})} n_{0i}^\mu(\mathbf{r}') n_{0i}^\mu(\mathbf{r}) \quad (94)$$

and

$$X^{(1)} = - \iint d\mathbf{r}d\mathbf{r}' \frac{\delta^2 E_{\text{Hxc}}^{\text{sr},\mu}[n^0]}{\delta n(\mathbf{r}')\delta n(\mathbf{r})} n_{0i}^\mu(\mathbf{r}) \times (E_0^{[2]\mu} - \omega^{(0)}S^{[2]\mu})^{-1} (n^{[1]\mu}(\mathbf{r}') - n_{0i}^\mu(\mathbf{r}')X^{(0)}), \quad (95)$$

respectively. Combining Eq. (85) with Eqs. (92) and (95) leads to the following expression for the second-order correction to

the excitation energy:

$$\omega^{(2)} = \iiint d\mathbf{r}_1 d\mathbf{r}'_1 d\mathbf{r}d\mathbf{r}' \frac{\delta^2 E_{\text{Hxc}}^{\text{sr},\mu}[n^0]}{\delta n(\mathbf{r}'_1)\delta n(\mathbf{r}_1)} \times \frac{\delta^2 E_{\text{Hxc}}^{\text{sr},\mu}[n^0]}{\delta n(\mathbf{r}')\delta n(\mathbf{r})} n_{0i}^\mu(\mathbf{r}) n_{0i}^\mu(\mathbf{r}') \times \left(\sum_{i>1} \frac{n_{0i}^\mu(\mathbf{r}_1) n_{0i}^\mu(\mathbf{r}')}{\mathcal{E}_1^\mu - \mathcal{E}_i^\mu} + \sum_{i\geq 1} \frac{n_{0i}^\mu(\mathbf{r}_1) n_{0i}^\mu(\mathbf{r}')}{2\mathcal{E}_0^\mu - \mathcal{E}_i^\mu - \mathcal{E}_1^\mu} \right). \quad (96)$$

The second summation in Eq. (96) is related to de-excitations. Within the Tamm-Dancoff approximation the latter will be dropped, thus leading to the following expansion through second order, according to Eqs. (91) and (94):

$$\tilde{\omega} = \mathcal{E}_1^\mu - \mathcal{E}_0^\mu + \iint d\mathbf{r}d\mathbf{r}' \frac{\delta^2 E_{\text{Hxc}}^{\text{sr},\mu}[n^0]}{\delta n(\mathbf{r}')\delta n(\mathbf{r})} n_{0i}^\mu(\mathbf{r}') n_{0i}^\mu(\mathbf{r}) + \iiint d\mathbf{r}_1 d\mathbf{r}'_1 d\mathbf{r}d\mathbf{r}' \frac{\delta^2 E_{\text{Hxc}}^{\text{sr},\mu}[n^0]}{\delta n(\mathbf{r}'_1)\delta n(\mathbf{r}_1)} \times \frac{\delta^2 E_{\text{Hxc}}^{\text{sr},\mu}[n^0]}{\delta n(\mathbf{r}')\delta n(\mathbf{r})} n_{0i}^\mu(\mathbf{r}) n_{0i}^\mu(\mathbf{r}') \sum_{i>1} \frac{n_{0i}^\mu(\mathbf{r}_1) n_{0i}^\mu(\mathbf{r}')}{\mathcal{E}_1^\mu - \mathcal{E}_i^\mu} + \dots \quad (97)$$

A direct comparison can then be made with the LIM2 excitation energy in Eq. (68). Thus we conclude that the LIM2 can be recovered through first and second orders in the short-range kernel from adiabatic TD range-separated DFT by applying, within the Tamm-Dancoff approximation, the substitutions,

$$n_{0i}^\mu(\mathbf{r}) \rightarrow \frac{1}{2}(n_{\psi_i}^\mu(\mathbf{r}) - n^0(\mathbf{r})) \quad (98)$$

and

$$\sum_{i>1} \frac{n_{0i}^\mu(\mathbf{r}_1) n_{0i}^\mu(\mathbf{r}')}{\mathcal{E}_1^\mu - \mathcal{E}_i^\mu} \rightarrow 2 \sum_{i\geq 1} \frac{n_{0i}^\mu(\mathbf{r}_1) n_{0i}^\mu(\mathbf{r}')}{\mathcal{E}_0^\mu - \mathcal{E}_i^\mu}, \quad (99)$$

respectively.

H. Generalization to higher excitations

Following Gross *et al.* [7], we introduce the generalized w -dependent ensemble energy

$$E_I^w = \frac{1 - wg_I}{M_{I-1}} \times \left(\sum_{K=0}^{I-1} g_K E_K \right) + wg_I E_I, \quad (100)$$

which is associated with the ensemble weights,

$$w_k = \begin{cases} \frac{1-wg_I}{M_{I-1}}, & 0 \leq k \leq M_{I-1} - 1, \\ w, & M_{I-1} \leq k \leq M_I - 1, \end{cases} \quad (101)$$

with

$$0 \leq w \leq \frac{1}{M_I}, \quad M_I = \sum_{L=0}^I g_L, \quad (102)$$

and $E_0 < E_1 < \dots < E_I$ are the $I + 1$ lowest energies with degeneracies $\{g_L\}_{0 \leq L \leq I}$. In the exact theory, the ensemble

energy is linear in w , with slope

$$\frac{dE_I^w}{dw} = g_I E_I - \frac{g_I}{M_{I-1}} \left(\sum_{K=0}^{I-1} g_K E_K \right), \quad (103)$$

thus leading to the following expression for the exact I th excitation energy:

$$\omega_I = E_I - E_0 = \frac{1}{g_I} \frac{dE_I^w}{dw} + \frac{1}{M_{I-1}} \sum_{K=1}^{I-1} g_K \omega_K. \quad (104)$$

The LIM excitation energy, which has been introduced in Eq. (51) for nondegenerate ground and first-excited states, can therefore be generalized by substituting the approximate first-order derivative (which may be both μ and w dependent) with its linear-interpolated value over the segment $[0, 1/M_I]$,

$$\frac{d\tilde{E}_I^{\mu,w}}{dw} \rightarrow M_I (\tilde{E}_I^{\mu,1/M_I} - \tilde{E}_I^{\mu,0}), \quad (105)$$

so that the I th LIM excitation energy can be defined as

$$\begin{aligned} \omega_{\text{LIM},I}^{\mu} &= \frac{M_I}{g_I} (\tilde{E}_I^{\mu,1/M_I} - \tilde{E}_{I-1}^{\mu,1/M_{I-1}}) \\ &+ \frac{1}{M_{I-1}} \sum_{K=1}^{I-1} g_K \omega_{\text{LIM},K}^{\mu}, \end{aligned} \quad (106)$$

where the equality $\tilde{E}_{I-1}^{\mu,1/M_{I-1}} = \tilde{E}_I^{\mu,0}$ has been used. In other words, the LIM simply consists in interpolating linearly the ensemble energy between equiensembles that are described at the WIDFA level of approximation.

III. COMPUTATIONAL DETAILS

Equations (45) and (51) as well as their generalizations to any ensemble of ground and excited states [see Eq. (106)] have been implemented in a development version of the DALTON program package [47,48]. For simplicity, we considered spin-projected (singlet) ensembles only. In the latter case, the GOK variational principle is simply formulated in the space of singlet states [15]. In practice, both singlet and triplet states have been computed, but for the latter (which can be identified easily in a CI calculation), the ensemble weights have been set to 0. Both the spin-independent short-range local density approximation [20,21] (srLDA) and the short-range Perdew-Burke-Ernzerhof-type [23] (srPBE) approximation have been used. Basis sets are aug-cc-pVQZ [49,50]. Orbital relaxation and long-range correlation effects have been treated self-consistently at the full CI level (FCI) in the basis of the (ground-state) HF short-range DFT orbitals. For Be, the $1s$ orbitals were kept inactive. Indeed, in the standard wavefunction limit ($\mu \rightarrow +\infty$), deviations from TD coupled cluster with singles and doubles excitation energies are $0.4 mE_h$ and $2.0 mE_h$ for the $2s \rightarrow 3s$ and $(2s)^2 \rightarrow (2p)^2$ excitations, respectively. Comparisons are made with standard TD-DFT using the LDA [51], PBE [52], and Coulomb attenuated Becke three-parameter Lee-Yang-Parr [53] (CAM-B3LYP) functionals. We investigated the following ensembles consisting of two singlet states: $\{1^1S, 2^1S\}$ for He and Be, $\{1^1\Sigma^+, 2^1\Sigma^+\}$ for the stretched HeH⁺ molecule, and $\{1^1\Sigma_g^+, 2^1\Sigma_g^+\}$ for H₂ at equilibrium and in stretched geometries. For Be, the four-state

ensemble $\{1^1S, 2^1S, 1^1D\}$ in A_g symmetry (1^1D is doubly degenerate) has also been considered in order to compute the $1^1S \rightarrow 1^1D$ excitation energy.

IV. RESULTS AND DISCUSSION

A. Effective derivative discontinuities

1. GOK-DFT results ($\mu = 0$) for He

Let us first focus on the GOK-LDA results ($\mu = 0$ limit) obtained for He. As shown in the top left-hand panel in Fig. 3, the variation of the auxiliary excitation energy with w is very similar to that obtained at the quasi-LDA level by Yang *et al.* (see Fig. 11 in Ref. [15]). An interesting feature, observed with both methods, is the minimum around $w = 0.01$. The derivation of the first-order derivative for the auxiliary excitation energy is presented in Appendix B. As readily seen from the expression in Eq. (B10), at $w = 0$, the derivative contains two terms. The first one, which is linear in the Hxc kernel, is expected to be positive due to the Hartree contribution. The second one is quadratic in the Hxc kernel and is negative (because of the denominator), exactly like conventional second-order contributions to the ground-state energy in many-body perturbation theory. The latter term might be large enough at $w = 0$ so that the auxiliary excitation energy decreases with increasing w . The linearity in w [last term on the right-hand side of Eq. (B10)] explains why that derivative becomes 0 and is then positive for larger w values. As the excitation energy increases, the denominator mentioned previously also increases. The derivative will therefore increase, thus leading to the positive curvature observed for the auxiliary excitation energy. All these features are essentially driven by the response of the auxiliary excited state to changes in the ensemble weight (not shown). Returning to the top panels in Fig. 3, we see that the minimum at $w = 0.01$ only appears when auxiliary energies are computed self-consistently. This is consistent with Eq. (B10), where the second (negative) term on the right-hand side describes the response of the KS orbitals to changes in the Hxc potential through the w -dependent ensemble density. When the latter term is neglected, the auxiliary excitation energy has a positive slope already at $w = 0$. For larger w values, self-consistency effects on the slope are reduced. Indeed, the response of the GOK orbitals is expected to be smaller as the auxiliary excitation energy increases. The large deviation of the non-self-consistent auxiliary excitation energy from the self-consistent one is due to the fact that, for the former, the ensemble density is constructed from the ground-state KS orbitals. Finally, we note that the self-consistent auxiliary excitation energy equals the reference FCI one around $w = 0.4$. A very similar result has been obtained at the quasi-LDA level by Yang *et al.* [15]. We also find that both the LDA and the PBE yield very similar results.

Let us now turn to the LIM excitation energy for $\mu = 0$. By construction, it is w independent, as in the exact theory. Note that the auxiliary excitation energy equals the LIM one for a w value that is slightly larger than $1/4$, thus showing that the ensemble energy is not strictly quadratic in w . Moreover, as expected from the analysis in Appendix C, the effect of self-consistency is much stronger on the auxiliary excitation

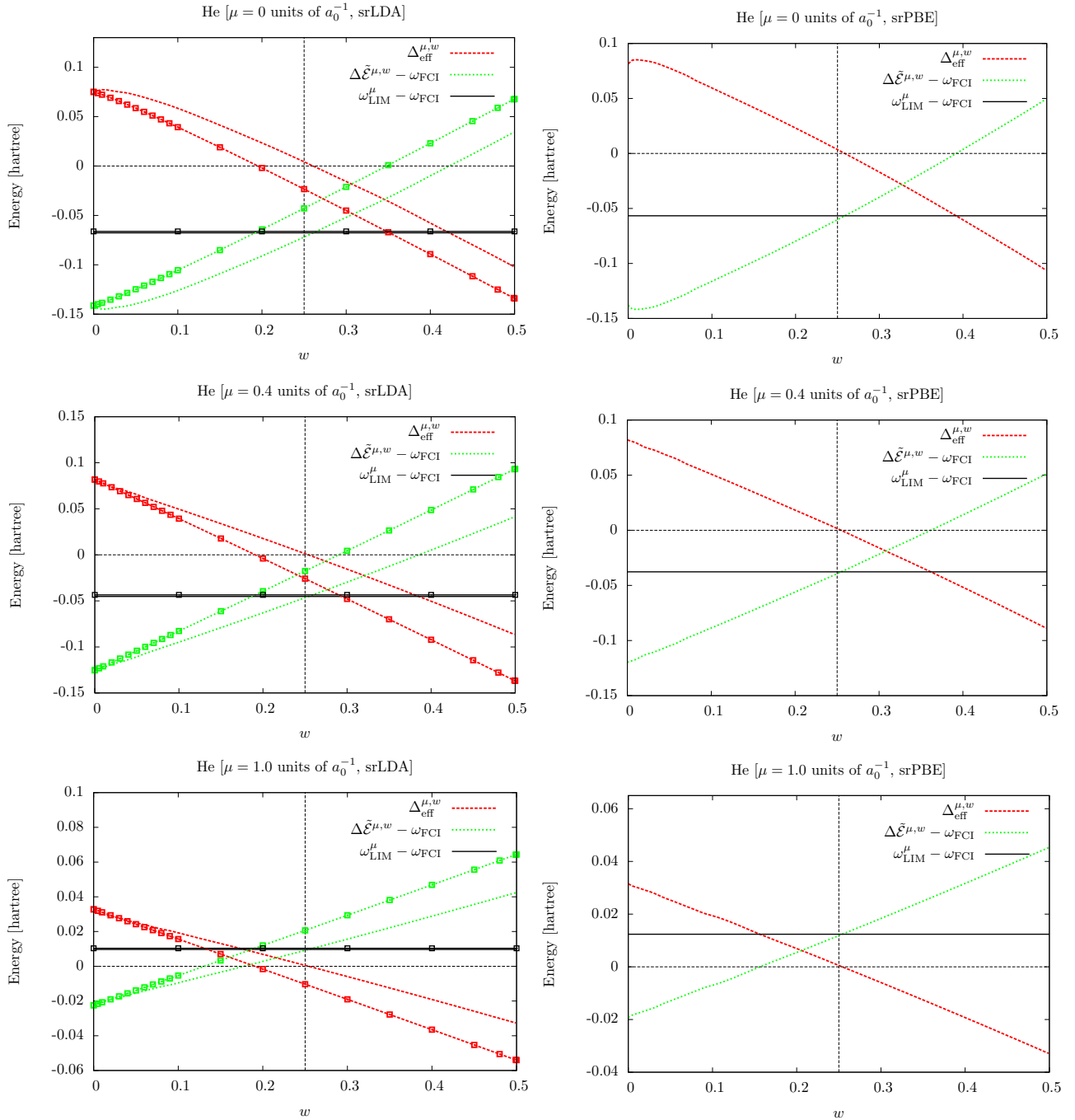


FIG. 3. (Color online) Effective DD ($\Delta_{\text{eff}}^{\mu,w}$), auxiliary ($\Delta\tilde{\mathcal{E}}^{\mu,w}$), and LIM ($\omega_{\text{LIM}}^{\mu}$) excitation energies associated with the excitation $1^1S \rightarrow 2^1S$ in He. Results are shown for $\mu = 0, 0.4a_0^{-1}$, and $1.0a_0^{-1}$ with the srLDA (left-hand panels) and srPBE (right-hand panels) functionals while varying the ensemble weight w . Comparison is made with the FCI excitation energy $\omega_{\text{FCI}} = 0.7668 E_h$. Open squares show non-self-consistent results.

energy than on the LIM one. For the latter it is actually negligible. Turning to the effective DDs in the top panels in Fig. 3, these vary with the ensemble weight, similarly to the accurate DD shown in Fig. 7 of Ref. [15]. Still, there are significant differences. For $w = 0$, the effective DD equals $0.0736E_h$ and $0.0814E_h$ at the LDA and PBE levels, respectively. The accurate value obtained by Yang *et al.* [15] is much smaller ($0.0116E_h$). In addition, both the LDA and the PBE effective DDs equal 0 close to $w = 1/4$, which is much

smaller than the accurate value of Ref. [15] ($w \approx 0.425$). Note, finally, that the substantial difference between the LIM and the FCI excitation energies prevents the effective DD and shifted auxiliary excitation energy curves from being symmetric with respect to the weight axis, as it should in the exact theory.

2. Range-separated results for He

As illustrated in the middle and bottom panels in Fig. 3, the auxiliary excitation energy, shown for $\mu = 0.4$ and $1.0a_0^{-1}$,

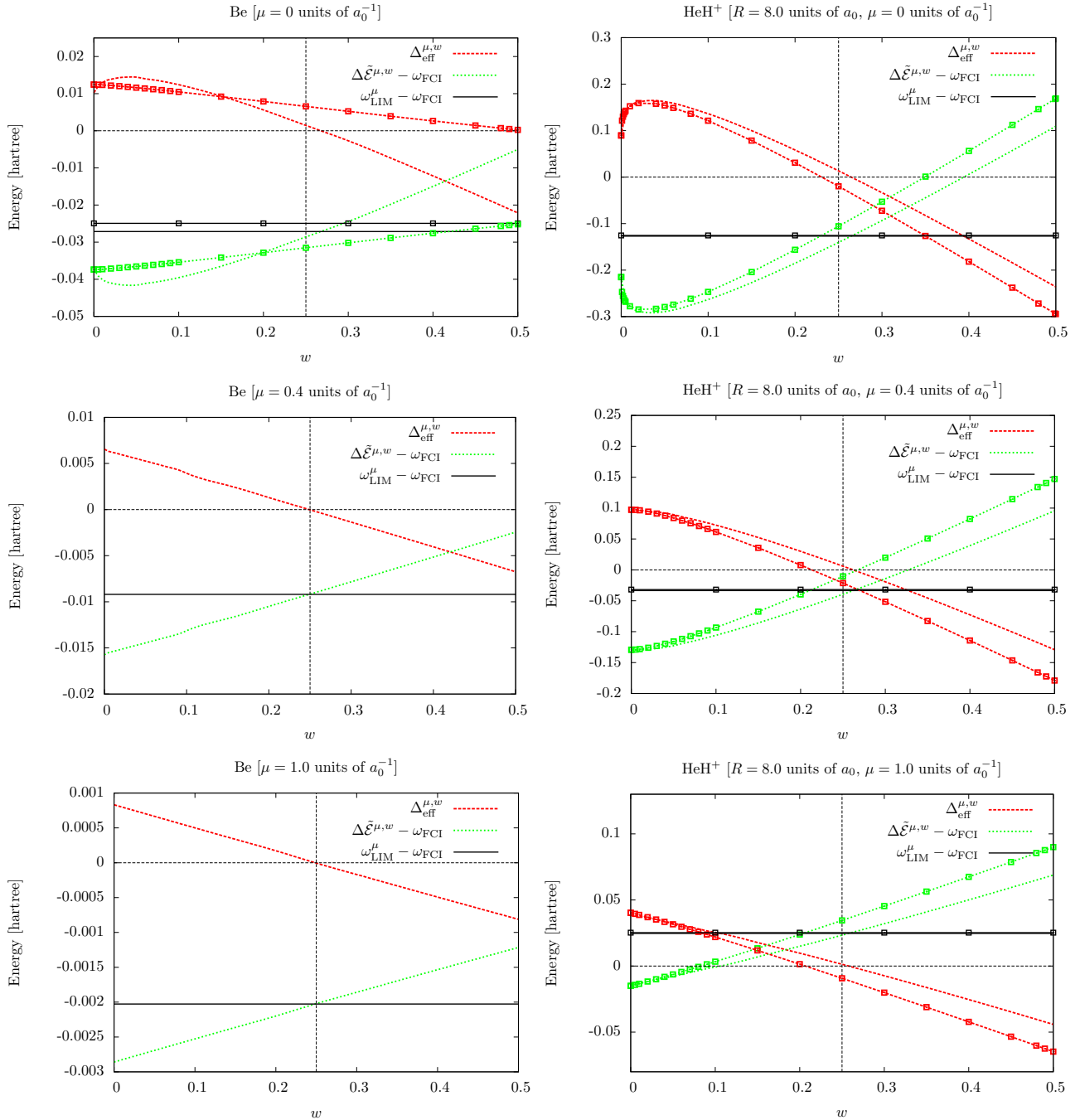


FIG. 4. (Color online) Effective DD ($\Delta_{\text{eff}}^{\mu,w}$), auxiliary ($\Delta\tilde{\mathcal{E}}^{\mu,w}$), and LIM ($\omega_{\text{LIM}}^{\mu}$) excitation energies associated with the excitations $1^1S \rightarrow 2^1S$ in Be (left-hand panels) and $1^1\Sigma^+ \rightarrow 2^1\Sigma^+$ in the stretched HeH⁺ molecule (right-hand panels). Results are shown for $\mu = 0, 0.4a_0^{-1}$, and $1.0a_0^{-1}$ with the srLDA functional while varying the ensemble weight w . Comparison is made with the FCI excitation energies ($\omega_{\text{FCI}} = 0.2487E_h$ for Be and $\omega_{\text{FCI}} = 0.4024E_h$ for HeH⁺). Open squares show non-self-consistent results.

becomes linear in w as μ increases. This is in agreement with the first-order derivative expression in Eq. (B7). Indeed, when $\mu \rightarrow +\infty$, the auxiliary wave functions become the physical ones which are w independent. Consequently, the third term on the right-hand side, which is responsible for the minimum at $w = 0.01$ observed when $\mu = 0$, vanishes for larger μ values. Similarly, the auxiliary energies will become w independent and equal to the physical energies, thus leading to a w -independent first-order derivative. Interestingly, the

(negative) second term on the right-hand side of Eq. (B7) is quadratic in the short-range kernel and is taken into account only when calculations are performed self-consistently. Since the short-range kernel becomes small as μ increases, it is not large enough to compensate the positive contribution from the first term, which is linear in the short-range kernel. As a result, the slope of the auxiliary excitation energy is positive for all w values. It also becomes clear that self-consistency will decrease the slope.

Turning to the LIM excitation energies and the effective DDs, the former become closer to the FCI value as μ increases while the latter are reduced, as expected. The fact that the auxiliary excitation energy equals the LIM one for $w = 0.25$ confirms that the range-separated ensemble energy is essentially quadratic in w when $\mu \geq 0.4a_0^{-1}$. Even though no accurate values for the short-range DD are available in the literature for any w , Fig. 2 in Ref. [37] provides reference values for $w = 0$ that are about $0.008E_h$ and $0.005E_h$ for $\mu = 0.4a_0^{-1}$ and $1.0a_0^{-1}$, respectively. These values are simply obtained by subtracting the auxiliary excitation energies (denoted $\Delta\mathcal{E}_k^\mu$ in Ref. [37]) from the standard FCI value ($\mu \rightarrow +\infty$ limit). The effective DDs computed at the srLDA level for $\mu = 0.4a_0^{-1}$ and $1.0a_0^{-1}$ differ from these reference values by about a factor of 10. Note that the srLDA and srPBE functionals give very similar results.

3. Be and the stretched HeH⁺ molecule

GOK-LDA and srLDA ($\mu = 0.4a_0^{-1}$ and $1.0a_0^{-1}$) results are presented for Be and the stretched HeH⁺ molecule in Fig. 4. In both systems, the ensemble contains the ground state and a first singly excited state, exactly as for He. Effective DD curves share similar patterns but their interpretations differ substantially. Let us first consider the Be atom. At the GOK-LDA level (top-left panel in Fig. 4), self-consistency effects are important. They are responsible for the negative slope of the auxiliary excitation energy at $w = 0$. Interestingly, the slope at $w = 0$ is larger in absolute value for He than for Be. This is clearly shown in the bottom panel in Fig. 5. As the auxiliary excitation energy decreases over a broader interval than for He, the second term on the right-hand side of Eq. (B10) might become larger in absolute value as w increases. Its combination with the third term (linear in w) may explain why the minimum is reached at a larger ensemble weight value than for He ($w \approx 0.045$). One may also argue that this third term, which is only described at the self-consistent level, is smaller for Be than for He, thus leading to a less pronounced curvature in w , as shown in the top panel in Fig. 5. The auxiliary excitation energy becomes linear in w when $\mu = 0.4a_0^{-1}$ and $1.0a_0^{-1}$ (see middle- and bottom-left panels in Fig. 4). Note, finally, that the effective DDs are about 10 times smaller than in He.

Let us now focus on the stretched HeH⁺ molecule. As shown in Fig. 5, patterns observed at the GOK-LDA level for He and Be are strongly enhanced due to the charge transfer. The interpretation is, however, quite different. Indeed, as shown in the top-right panel in Fig. 4, self-consistency is negligible for small w values and is therefore not responsible for the large negative slope of the auxiliary excitation energy at $w = 0$. This was expected since the self-consistent contribution to the slope [second term on the right-hand side of Eq. (B10)] involves the overlap between the HOMO (localized on He) and the LUMO, which is, in this particular case, strictly zero. Consequently, as clearly shown in Eq. (B12), the (negative) LDA exchange and correlation kernels [3] are responsible for the negative slope at $w = 0$. The latter is actually smaller in absolute value when the LDA correlation density functional is set to 0 in the calculation (not shown), thus confirming the importance of both exchange and correlation contributions to the kernel. Note that, as w increases, self-consistency effects

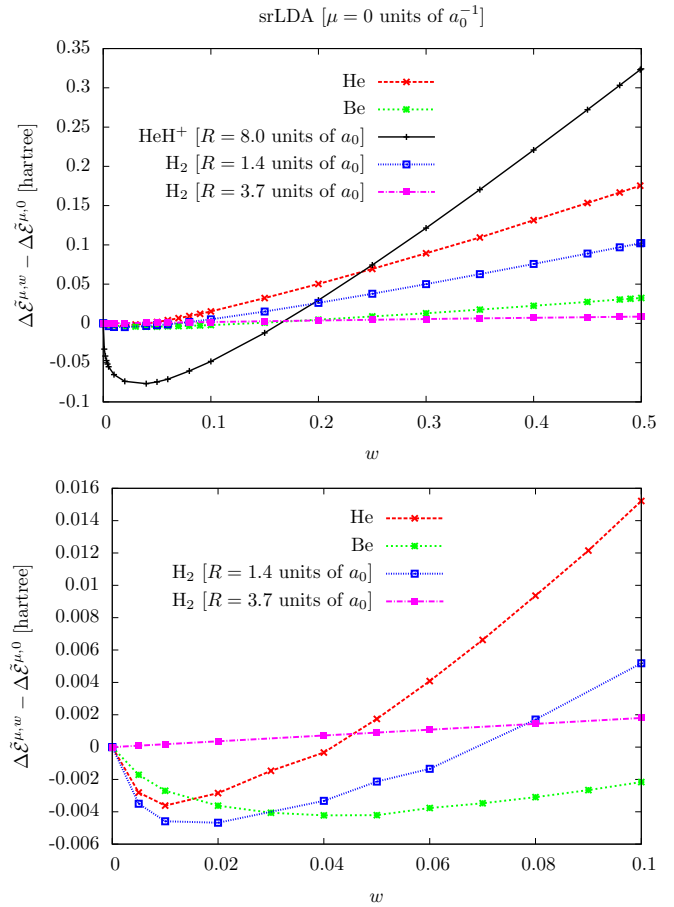


FIG. 5. (Color online) Auxiliary excitation energies obtained with $\mu = 0a_0^{-1}$ and the srLDA functional (which is equivalent to GOK-LDA) while varying the ensemble weight w in the various systems considered in this work. See text for further details. Excitation energies are shifted by their values at $w = 0$ for ease of comparison. Bottom: Zoom-in on the $0 \leq w \leq 0.1$ region.

increase. This can be related to the third term on the right-hand side of Eq. (B10), where the response of the excited state to changes in w contributes. Interestingly, for $\mu = 0.4a_0^{-1}$, the contribution to the slope, at $w = 0$, from the short-range xc kernel is significant enough [3] so that the pattern observed at the GOK-LDA level does not completely disappear (see the middle-right panel in Fig. 4). On the other hand, for the larger, $\mu = 1.0a_0^{-1}$ value, the auxiliary excitation energy becomes essentially linear in w with a positive slope (see the bottom-right panel in Fig. 4). Note, finally, that the stretched HeH⁺ molecule exhibits the largest effective DDs.

4. H₂

Results obtained for H₂ are shown in Figs. 5 and 6. At equilibrium, they are quite similar to those obtained for He. Still, at the GOK-LDA level, the negative slope of the auxiliary excitation energy at $w = 0$ is not related to the self-consistency (see the top-left panel in Fig. 6), in contrast to He. Self-consistency effects become significant as w increases. Effective DDs at $w = 0$ are equal to $40.9 mE_h$, $36.2 mE_h$, and $8.6 mE_h$ for $\mu = 0, 0.4a_0^{-1}$, and $1.0a_0^{-1}$, respectively. They

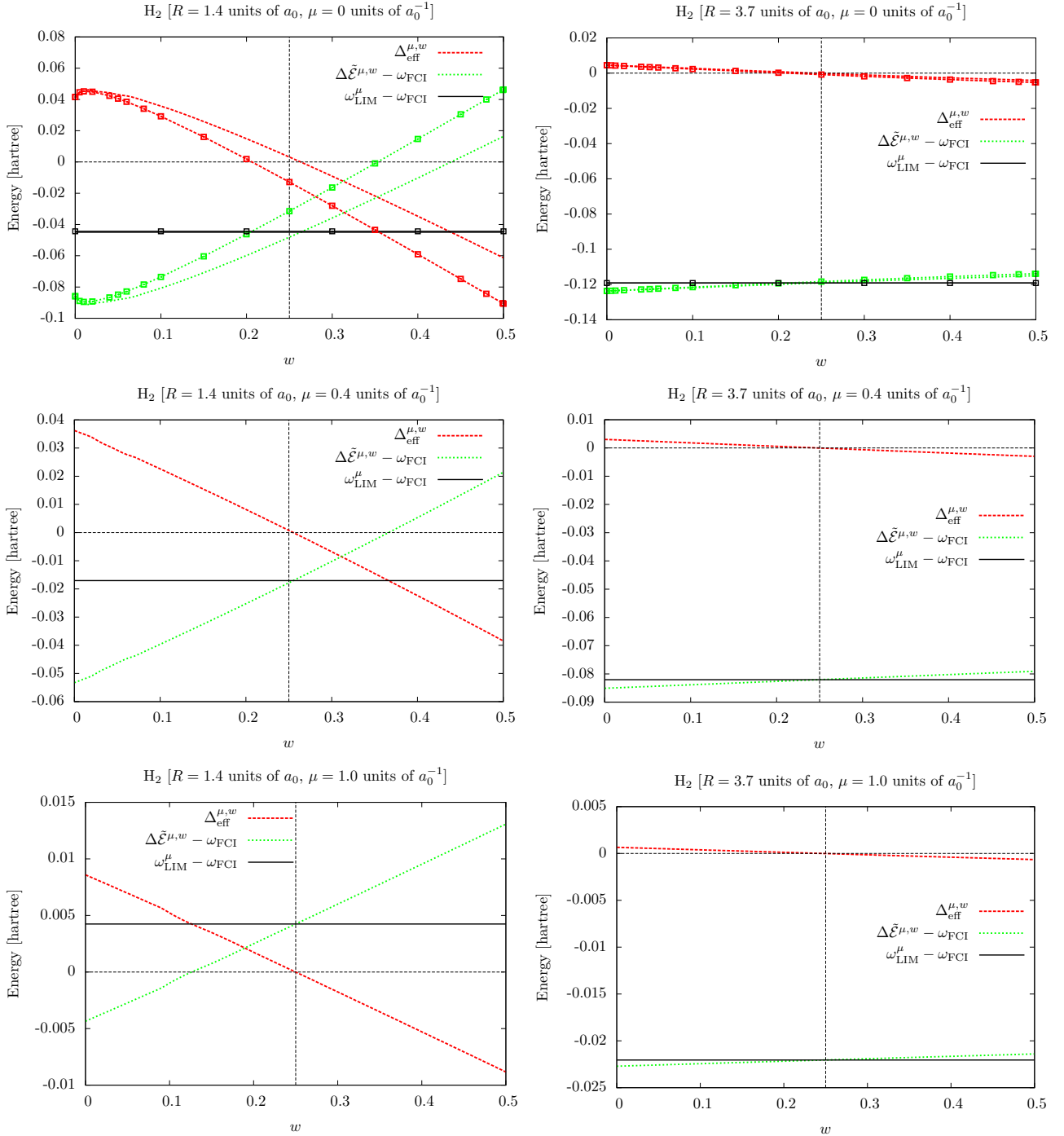


FIG. 6. (Color online) Effective DD ($\Delta_{\text{eff}}^{\mu,w}$), auxiliary ($\Delta\tilde{\mathcal{E}}^{\mu,w}$), and LIM ($\omega_{\text{LIM}}^{\mu}$) excitation energies associated with the excitation $1^1\Sigma_g^+ \rightarrow 2^1\Sigma_g^+$ in H_2 at equilibrium (left-hand panels) and in the stretched geometry (right-hand panels). Results are shown for $\mu = 0, 0.4a_0^{-1}$, and $1.0a_0^{-1}$ with the srLDA functional while varying the ensemble weight w . Comparison is made with the FCI excitation energies ($\omega_{\text{FCI}} = 0.4828E_h$ at equilibrium and $\omega_{\text{FCI}} = 0.3198E_h$ in the stretched geometry). Open squares show non-self-consistent results.

are significantly larger than the accurate values deduced from Fig. 6 in Ref. [37] ($7.1 mE_h$, $5.7 mE_h$, and about 0).

In the stretched geometry (right-hand panels in Fig. 6), the nature of the first excited state completely changes. It corresponds to the double excitation $1\sigma_g^2 \rightarrow 1\sigma_u^2$. At the GOK-LDA level, self-consistency effects are negligible. This was expected since, according to Eq. (B7), the latter effects involve couplings between ground and excited states through

the density operator. Consequently, a doubly excited state will not contribute. Moreover, the difference in densities between the ground-state and the first doubly excited GOK determinants decreases along the bond-breaking coordinate, simply because the overlap between the $1s$ orbitals decreases. As a result, the first-order derivative of the auxiliary excitation energy is very small, as confirmed by Fig. 5. This analysis holds also for larger μ values. The only difference is that,

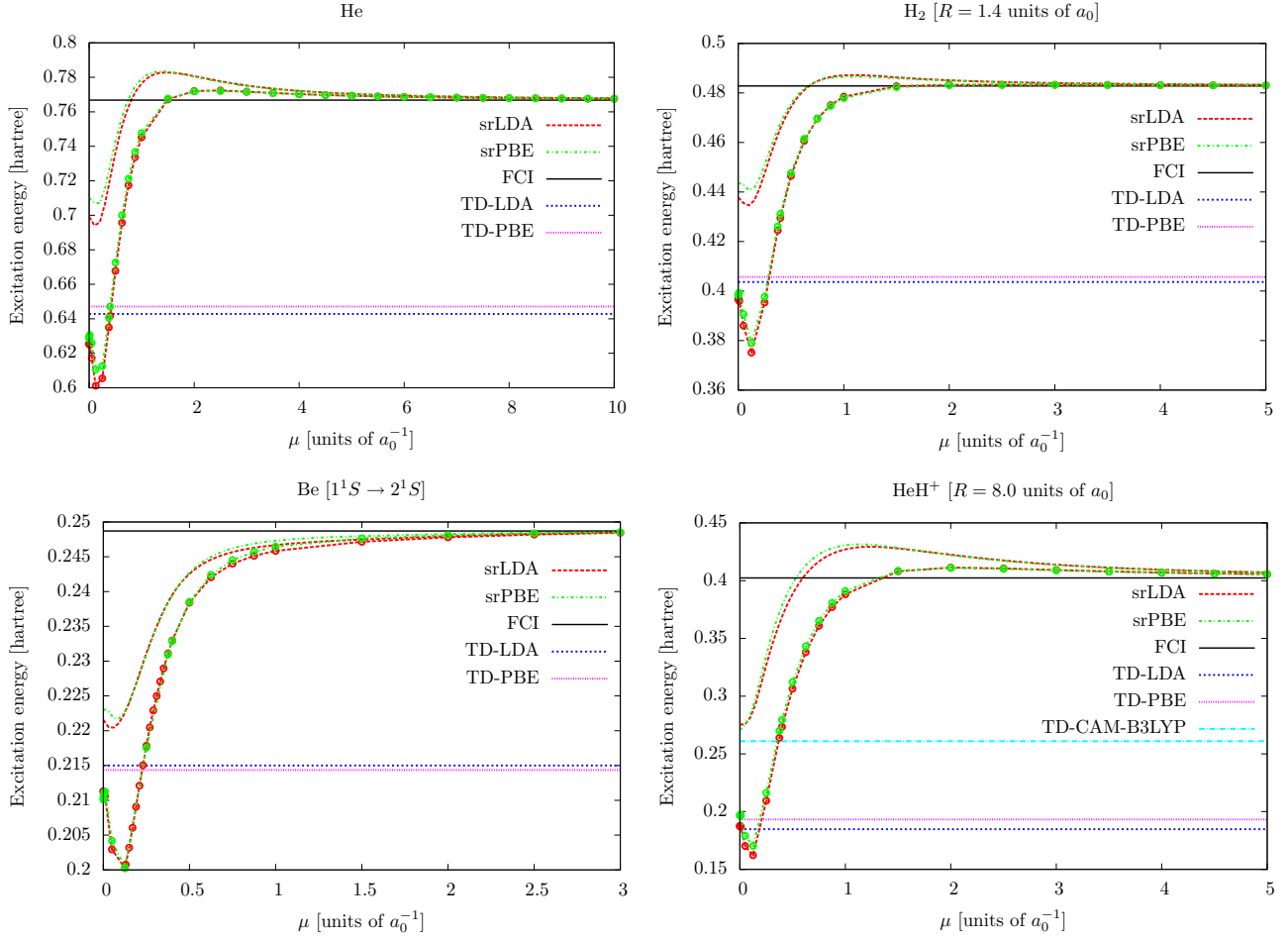


FIG. 7. (Color online) LIM excitation energies obtained for the single excitations discussed in this work with srLDA and srPBE functionals while varying the range-separation parameter μ . Comparison is made with the standard TD-DFT and FCI. For analysis purposes, auxiliary excitation energies obtained from the ground-state density ($w = 0$) are shown (curves with open circles).

when $\mu > 0$, both ground- and excited-state wave functions are multiconfigurational [54,55]. In a minimal basis, they are simply written as

$$\begin{aligned} |\Psi_0^\mu\rangle &= \frac{1}{\sqrt{2}}(|\sigma_g^2\rangle - |\sigma_u^2\rangle), \\ |\Psi_1^\mu\rangle &= \frac{1}{\sqrt{2}}(|\sigma_g^2\rangle + |\sigma_u^2\rangle). \end{aligned} \quad (107)$$

In this case, both ground and excited states have the same density,

$$n_{\Psi_0^\mu}(\mathbf{r}) = n_{\Psi_1^\mu}(\mathbf{r}) = \frac{1}{2}(n_{\sigma_g^2}(\mathbf{r}) + n_{\sigma_u^2}(\mathbf{r})), \quad (108)$$

and their coupling through the density operator equals

$$\langle \Psi_0^\mu | \hat{n}(\mathbf{r}) | \Psi_1^\mu \rangle = \frac{1}{2}(n_{\sigma_g^2}(\mathbf{r}) - n_{\sigma_u^2}(\mathbf{r})), \quad (109)$$

which is 0, as the overlap between the $1s$ orbitals is neglected.

Since the ensemble energy is, for any μ value, almost linear in w , the LIM and auxiliary excitation energies are very close for any weight. Consequently, the effective DD is very small ($4.5 mE_h$ for $\mu = 0a_0^{-1}$ and $w = 0$). Since the deviation of the LIM excitation energy from the FCI one is relatively large (about $-0.12E_h$ for $\mu = 0a_0^{-1}$), the symmetry of the plotted curves with respect to the weight axis is completely broken,

in contrast to the other systems. In this particular situation, LIM brings no improvement and the effective DD is expected to be far from the true DD. For comparison, the latter equals about $200 mE_h$ for a slightly larger bond distance ($4.2a_0$) and $\mu = 0a_0^{-1}$, according to Fig. 7 in Ref. [37]. For the same distance, the KS-LDA auxiliary excitation energy (not shown) deviates by $130 mE_h$ in absolute value from the FCI value, which is of the same order of magnitude as the true DD. Therefore, for $R = 3.7a_0$, the true DD is expected to be much larger than the effective one.

B. Excitation energies

1. Single excitations

LIM excitation energies have been computed when varying μ for the various systems studied previously. Single excitations are discussed in this section. Results are shown in Fig. 7. It is quite remarkable that, already for $\mu = 0$, the LIM performs better than the standard TD-DFT with the same functional (LDA or PBE). This is also true for the $2\Sigma^+$ charge transfer state in the stretched HeH⁺ molecule. We even obtain slightly better results than with the popular TD-CAM-B3LYP method. As expected, the error with respect to FCI decreases as μ increases. Note that, for He, it becomes 0 and then changes

sign in the vicinity of $\mu = 1.0a_0^{-1}$. The latter value also gives accurate results for the other systems, which is in agreement with Ref. [13]. Note also that, for the typical value $\mu = 0.4a_0^{-1}$ to $0.5a_0^{-1}$ [25,26], the slope in μ for the LIM excitation energy is quite significant. It would therefore be relevant to adapt the extrapolation scheme of Savin [36,38] to range-separated ensemble DFT. This is left for future work. Note that the srLDA and srPBE functionals give rather similar results. For comparison, auxiliary excitation energies obtained from the ground-state density ($w = 0$) are also shown. The former are equal to KS orbital energy differences when $\mu = 0$. In this case, TD-DFT gives slightly better results, except for the charge transfer excitation in HeH^+ , where the difference is very small, as expected [1]. Both srLDA and srPBE auxiliary excitation energies reach a minimum at relatively small μ values ($0.125a_0^{-1}$ for He). This is due to the approximate short-range (semi-)local potentials that we used. Indeed, as shown in Ref. [37], variations in μ are expected to be monotonic for He and H_2 at equilibrium if an accurate short-range potential is used. Since the range-separated ensemble energy can be expressed in terms of the auxiliary energies [see Eq. (47)], it is not surprising to recover such minima for some LIM excitation energies. Let us, finally, note that the auxiliary excitation energy converges more rapidly than the LIM one to the FCI value when μ increases from $1.0a_0^{-1}$. For Be, convergences are very similar. As already mentioned, the convergence can actually be further improved by means of extrapolation techniques [36,38]. In conclusion, the LIM approach is promising at both GOK-DFT and range-separated ensemble DFT levels. In the latter case, μ should not be too large; otherwise the use of an ensemble is less relevant. Indeed, auxiliary excitation energies obtained from the ground-state density are in fact better approximations to the FCI excitation energies, at least for the systems and approximate short-range functionals considered in this work. This should be tested on more systems in the future.

2. Double excitations

One important feature of both GOK and range-separated ensemble DFT is the possibility of modeling multiple excitations, in contrast to standard TD-DFT. Results obtained for the $2^1\Sigma_g^+$ and 1^1D states in the stretched H_2 molecule and Be, respectively, are shown in Fig. 8. We focus on H_2 first. As discussed previously, LIM and auxiliary excitation energies are almost identical in this case. For $\mu = 0a_0^{-1}$, they differ by about $-0.12E_h$ from the FCI value. There are no significant differences between srLDA and srPBE results. The error monotonically decreases with increasing μ . Interestingly, for $\mu = 0.4a_0^{-1}$, the LIM excitation energy equals $0.237E_h$, which is very similar to the multiconfiguration range-separated TD-DFT result obtained with the same functionals ($0.238E_h$). [4] This confirms that the short-range kernel does not contribute significantly to the excitation energy, since the ground and doubly excited states are not coupled by the density operator [see Eq. (109)]. Note that, for $R = 4.2a_0$ and $\mu = 0.4a_0^{-1}$, the srLDA auxiliary excitation energy (not shown) equals $0.194E_h$, which is rather close to the accurate value ($0.181E_h$) deduced from Fig. 7 in Ref. [37]. As a result, the approximate (semi-)local density-functional potentials are not responsible

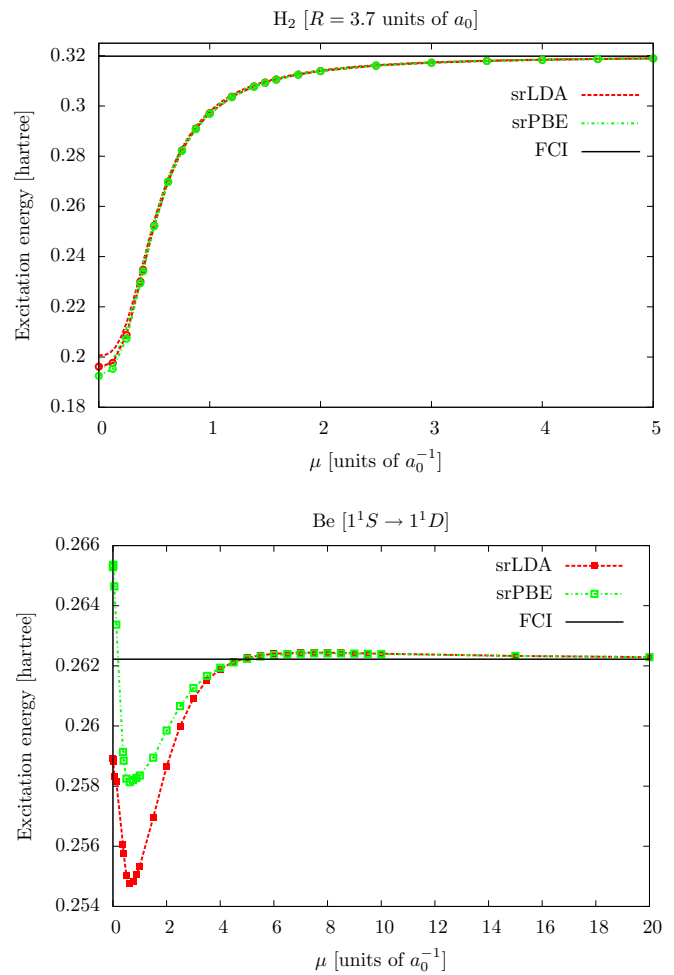


FIG. 8. (Color online) LIM excitation energies calculated for the doubly excited $2^1\Sigma_g^+$ state in the stretched H_2 molecule (top panel) and the 1^1D state in Be (bottom panel) while varying the range-separation parameter μ with srLDA and srPBE functionals. Comparison is made with the FCI. For H_2 , auxiliary excitation energies obtained from the ground-state density ($w = 0$) are shown (curves with open circles) for comparison.

for the large error in the excitation energy. One would blame the adiabatic approximation if TD linear response theory were used. In our case, it is related to the WIDFA approach. In this respect, it seems essential to develop weight-dependent xc functionals for ensembles. Applying the generalized adiabatic connection formalism for ensembles to model systems would be instructive in that respect. Work is currently in progress in this direction.

Turning to the doubly excited 1^1D state in Be, the LIM is quite accurate already at the GOK-DFT level. Interestingly, the largest and relatively small errors in absolute value (about $4.0\text{ m}E_h$ and $7.0\text{ m}E_h$ for the srLDA and srPBE functionals, respectively) are obtained around $\mu = 1.0a_0^{-1}$. In this case, the ensemble contains four states (1^1S , 2^1S , and two degenerate 1^1D states), whereas in all previous cases first excitation energies were computed with only two states. This indicates that μ values that are optimal in terms of accuracy may depend on the choice of the ensemble. This should be investigated further in the future.

V. CONCLUSIONS

A rigorous combination of wave-function theory with ensemble DFT for excited states has been investigated by means of range separation. As illustrated for simple two- and four-electron systems, using local or semilocal ground-state density-functional approximations for modeling the short-range xc energy of a biensemble with weight w usually leads to range-separated ensemble energies that are not strictly linear in w . Consequently, the approximate excitation energy, which is defined as the derivative of the ensemble energy with respect to w , becomes w dependent, unlike the exact derivative. Moreover, the variation in w can be very sensitive to the self-consistency effects that are induced by the short-range density-functional potential.

In order to define unambiguously approximate excitation energies in this context, we have proposed a LIM that simply interpolates the ensemble energy between $w = 0$ (ground state) and $w = 1/2$ (equiensemble consisting of the nondegenerate ground and first excited states). A generalization to higher excitations with degenerate ground and excited states has been formulated and tested. It simply consists in interpolating the ensemble energy linearly between equiensembles. The LIM is applicable to the GOK-DFT, which is recovered when the range-separation parameter μ equals 0. In the latter case, the LIM performs systematically better than the standard TD-DFT with the same functional, even for the $2\Sigma^+$ charge-transfer state in the stretched HeH^+ molecule. For typical values $\mu = 0.4a_0^{-1}$ to $0.5a_0^{-1}$, the LIM gives a better approximation to the excitation energy than the auxiliary long-range-interacting one obtained from the ground-state density. However, for larger μ values, the latter excitation energy usually converges to the physical result more rapidly than the LIM one.

One of the motivations for using ensembles is the possibility, in contrast to the standard TD-DFT, of modeling double excitations. Results obtained with the LIM for the 1^1D state in Be are relatively accurate, especially at the GOK-DFT level. In the particular case of the stretched H_2 molecule, the range-separated ensemble energy is almost linear in w , thus making the approximate $2^1\Sigma_g^+$ excitation energy almost weight independent. The LIM does not improve on that case and the error on the excitation energy is quite significant. This example illustrates the need for weight-dependent xc functionals. Combining adiabatic connection formalisms [14] with accurate reference data [15] will hopefully enable the development of density-functional approximations for ensembles in the near-future.

Finally, in order to turn the LIM into a useful modeling tool, a state-averaged complete active space self-consistent field should be used rather than the CI for the computation of long-range correlation effects. Since the long-range interaction has no singularity at $r_{12} = 0$, we expect a limited number of configurations to be sufficient for recovering most of the long-range correlation. This observation has already been made for the ground state [33,56]. Obviously, the active space should be chosen carefully in order to preserve size consistency. The implementation and calibration of such a method is left for future work.

ACKNOWLEDGMENTS

E.F. thanks Alex Borgoo and Laurent Mazouin for fruitful discussions. The authors would like to dedicate the paper to the memory of Prof. Tom Ziegler who supported this work on ensemble DFT and contributed significantly in recent years to the development of time-independent DFT for excited states. E.F. acknowledges financial support from LABEX ‘‘Chemistry of complex systems’’ and ANR (MCFUNEX project).

APPENDIX A: SELF-CONSISTENT RANGE-SEPARATED ENSEMBLE DENSITY-FUNCTIONAL PERTURBATION THEORY

The self-consistent Eq. (45) can be solved for small w values within perturbation theory. For that purpose we partition the long-range interacting density-functional Hamiltonian as

$$\hat{H}^\mu[\tilde{n}^{\mu,w}] = \hat{H}^\mu[n^0] + w\hat{\mathcal{V}}^{\mu,w}, \quad (\text{A1})$$

where, according to Eq. (9), the perturbation equals

$$w\hat{\mathcal{V}}^{\mu,w} = \int d\mathbf{r} \left(\frac{\delta E_{\text{Hxc}}^{\text{sr},\mu}[\tilde{n}^{\mu,w}]}{\delta n(\mathbf{r})} - \frac{\delta E_{\text{Hxc}}^{\text{sr},\mu}[n^0]}{\delta n(\mathbf{r})} \right) \hat{n}(\mathbf{r}), \quad (\text{A2})$$

and according to Eq. (44),

$$\begin{aligned} \tilde{n}^{\mu,w}(\mathbf{r}) &= n^0(\mathbf{r}) + w \left. \frac{\partial \tilde{n}^{\mu,w}(\mathbf{r})}{\partial w} \right|_{w=0} + O(w^2) \\ &= n^0(\mathbf{r}) + w(n_{\Psi_1^\mu}(\mathbf{r}) - n^0(\mathbf{r})) \\ &\quad + w \left. \frac{\partial n_{\tilde{\Psi}_0^{\mu,w}}(\mathbf{r})}{\partial w} \right|_{w=0} + O(w^2). \end{aligned} \quad (\text{A3})$$

Combining Eq. (A2) with Eq. (A3) leads to

$$\begin{aligned} \hat{\mathcal{V}}^{\mu,w} &= \hat{\mathcal{V}}^{\mu,0} + O(w) \\ &= \iint d\mathbf{r}d\mathbf{r}' \frac{\delta^2 E_{\text{Hxc}}^{\text{sr},\mu}[n^0]}{\delta n(\mathbf{r}')\delta n(\mathbf{r})} \left(n_{\Psi_1^\mu}(\mathbf{r}') - n^0(\mathbf{r}') \right. \\ &\quad \left. + \left. \frac{\partial n_{\tilde{\Psi}_0^{\mu,w}}(\mathbf{r}')}{\partial w} \right|_{w=0} \right) \hat{n}(\mathbf{r}) + O(w). \end{aligned} \quad (\text{A4})$$

From the usual first-order wave-function correction expression,

$$\left| \frac{\partial \tilde{\Psi}_0^{\mu,w}}{\partial w} \right|_{w=0} = \sum_{i \geq 1} |\Psi_i^\mu\rangle \frac{\langle \Psi_i^\mu | \hat{\mathcal{V}}^{\mu,0} | \Psi_0^\mu \rangle}{\mathcal{E}_0^\mu - \mathcal{E}_i^\mu}, \quad (\text{A5})$$

and the expression for the derivative of the ground-state density, which we simply denote ∂n^μ ,

$$\partial n^\mu(\mathbf{r}_1) = \left. \frac{\partial n_{\tilde{\Psi}_0^{\mu,w}}(\mathbf{r}_1)}{\partial w} \right|_{w=0} = 2 \langle \Psi_0^\mu | \hat{n}(\mathbf{r}_1) \left| \frac{\partial \tilde{\Psi}_0^{\mu,w}}{\partial w} \right|_{w=0} \rangle, \quad (\text{A6})$$

we obtain the self-consistent equation

$$\partial n^\mu = \hat{\mathcal{F}} \partial n^\mu + \hat{\mathcal{F}}(n_{\Psi_1^\mu} - n^0), \quad (\text{A7})$$

where $\hat{\mathcal{F}}$ is a linear operator that acts on any function $f(\mathbf{r})$ as follows:

$$\hat{\mathcal{F}}f(\mathbf{r}_1) = 2 \sum_{i \geq 1} \iint d\mathbf{r} d\mathbf{r}' \frac{\delta^2 E_{\text{Hxc}}^{\text{sr},\mu}[n^0]}{\delta n(\mathbf{r}') \delta n(\mathbf{r})} \frac{n_{0i}^\mu(\mathbf{r}_1) n_{0i}^\mu(\mathbf{r})}{\mathcal{E}_0^\mu - \mathcal{E}_i^\mu} f(\mathbf{r}'),$$

$$n_{0i}^\mu(\mathbf{r}) = \langle \Psi_0^\mu | \hat{n}(\mathbf{r}) | \Psi_i^\mu \rangle. \quad (\text{A8})$$

Consequently,

$$\begin{aligned} \partial n^\mu &= (1 - \hat{\mathcal{F}})^{-1} \hat{\mathcal{F}}(n_{\Psi_1^\mu} - n^0) \\ &= \sum_{k=0}^{+\infty} \hat{\mathcal{F}}^k \hat{\mathcal{F}}(n_{\Psi_1^\mu} - n^0) = \hat{\mathcal{F}}(n_{\Psi_1^\mu} - n^0) + \dots \end{aligned} \quad (\text{A9})$$

APPENDIX B: DERIVATIVE OF THE AUXILIARY EXCITATION ENERGY

According to Eq. (48), the first-order derivative of the individual auxiliary energies can be expressed as

$$\frac{d\tilde{\mathcal{E}}_i^{\mu,w}}{dw} = \iint d\mathbf{r}' d\mathbf{r} \frac{\delta^2 E_{\text{Hxc}}^{\text{sr},\mu}[\tilde{n}^{\mu,w}]}{\delta n(\mathbf{r}') \delta n(\mathbf{r})} \frac{\partial \tilde{n}^{\mu,w}(\mathbf{r}')}{\partial w} n_{\tilde{\Psi}_i^{\mu,w}}(\mathbf{r}), \quad (\text{B1})$$

where

$$\frac{\partial \tilde{n}^{\mu,w}(\mathbf{r}')}{\partial w} = \delta \tilde{n}^{\mu,w}(\mathbf{r}') + \frac{\partial n_{\tilde{\Psi}_0^{\mu,w}}(\mathbf{r}')}{\partial w} + w \frac{\partial \delta \tilde{n}^{\mu,w}(\mathbf{r}')}{\partial w} \quad (\text{B2})$$

and

$$\delta \tilde{n}^{\mu,w}(\mathbf{r}') = n_{\tilde{\Psi}_1^{\mu,w}}(\mathbf{r}') - n_{\tilde{\Psi}_0^{\mu,w}}(\mathbf{r}'), \quad (\text{B3})$$

so that the derivative of the auxiliary excitation energy in Eq. (49) can be written as

$$\begin{aligned} \frac{d\Delta \tilde{\mathcal{E}}^{\mu,w}}{dw} &= \iint d\mathbf{r}' d\mathbf{r} \frac{\delta^2 E_{\text{Hxc}}^{\text{sr},\mu}[\tilde{n}^{\mu,w}]}{\delta n(\mathbf{r}') \delta n(\mathbf{r})} \\ &\quad \times \left(\delta \tilde{n}^{\mu,w}(\mathbf{r}') \delta \tilde{n}^{\mu,w}(\mathbf{r}) + \frac{\partial n_{\tilde{\Psi}_0^{\mu,w}}(\mathbf{r}')}{\partial w} \delta \tilde{n}^{\mu,w}(\mathbf{r}) \right. \\ &\quad \left. + w \frac{\partial \delta \tilde{n}^{\mu,w}(\mathbf{r}')}{\partial w} \delta \tilde{n}^{\mu,w}(\mathbf{r}) \right). \end{aligned} \quad (\text{B4})$$

According to perturbation theory through first order (see Appendix A), the response of the ground-state density to variations in the ensemble weight equals

$$\begin{aligned} \frac{\partial n_{\tilde{\Psi}_0^{\mu,w}}(\mathbf{r}')}{\partial w} &= 2 \langle \tilde{\Psi}_0^{\mu,w} | \hat{n}(\mathbf{r}') | \frac{\partial \tilde{\Psi}_0^{\mu,w}}{\partial w} \rangle \\ &= 2 \sum_{i \geq 1} \iint d\mathbf{r}_1 d\mathbf{r}_2 \frac{\delta^2 E_{\text{Hxc}}^{\text{sr},\mu}[\tilde{n}^{\mu,w}]}{\delta n(\mathbf{r}_2) \delta n(\mathbf{r}_1)} \\ &\quad \times \frac{n_{0i}^{\mu,w}(\mathbf{r}') n_{0i}^{\mu,w}(\mathbf{r}_1) \partial \tilde{n}^{\mu,w}(\mathbf{r}_2)}{\tilde{\mathcal{E}}_0^{\mu,w} - \tilde{\mathcal{E}}_i^{\mu,w}} \frac{1}{\partial w}, \end{aligned} \quad (\text{B5})$$

where $n_{0i}^{\mu,w}(\mathbf{r}') = \langle \tilde{\Psi}_0^{\mu,w} | \hat{n}(\mathbf{r}') | \tilde{\Psi}_i^{\mu,w} \rangle$. Note that, as pointed out for $w=0$ [see Eq. (A7)], Eq. (B5) should be solved self-consistently. By considering the first contribution to the response of the ensemble density in Eq. (B2)

we obtain

$$\begin{aligned} \frac{\partial n_{\tilde{\Psi}_0^{\mu,w}}(\mathbf{r}')}{\partial w} &= 2 \sum_{i \geq 1} \iint d\mathbf{r}_1 d\mathbf{r}_2 \frac{\delta^2 E_{\text{Hxc}}^{\text{sr},\mu}[\tilde{n}^{\mu,w}]}{\delta n(\mathbf{r}_2) \delta n(\mathbf{r}_1)} \\ &\quad \times \frac{n_{0i}^{\mu,w}(\mathbf{r}') n_{0i}^{\mu,w}(\mathbf{r}_1)}{\tilde{\mathcal{E}}_0^{\mu,w} - \tilde{\mathcal{E}}_i^{\mu,w}} \delta \tilde{n}^{\mu,w}(\mathbf{r}_2) + \dots, \end{aligned} \quad (\text{B6})$$

thus leading to the following expansion:

$$\begin{aligned} \frac{d\Delta \tilde{\mathcal{E}}^{\mu,w}}{dw} &= \iint d\mathbf{r}' d\mathbf{r} \frac{\delta^2 E_{\text{Hxc}}^{\text{sr},\mu}[\tilde{n}^{\mu,w}]}{\delta n(\mathbf{r}') \delta n(\mathbf{r})} \delta \tilde{n}^{\mu,w}(\mathbf{r}') \delta \tilde{n}^{\mu,w}(\mathbf{r}) \\ &\quad + 2 \sum_{i \geq 1} \frac{1}{\tilde{\mathcal{E}}_0^{\mu,w} - \tilde{\mathcal{E}}_i^{\mu,w}} \\ &\quad \times \left(\iint d\mathbf{r}' d\mathbf{r} \frac{\delta^2 E_{\text{Hxc}}^{\text{sr},\mu}[\tilde{n}^{\mu,w}]}{\delta n(\mathbf{r}') \delta n(\mathbf{r})} \delta \tilde{n}^{\mu,w}(\mathbf{r}') n_{0i}^{\mu,w}(\mathbf{r}') \right)^2 \\ &\quad + w \left(\iint d\mathbf{r}' d\mathbf{r} \frac{\delta^2 E_{\text{Hxc}}^{\text{sr},\mu}[\tilde{n}^{\mu,w}]}{\delta n(\mathbf{r}') \delta n(\mathbf{r})} \frac{\partial \delta \tilde{n}^{\mu,w}(\mathbf{r}')}{\partial w} \delta \tilde{n}^{\mu,w}(\mathbf{r}) \right) \\ &\quad + \dots \end{aligned} \quad (\text{B7})$$

Note that, at the srLDA level of approximation, the xc contribution to the short-range kernel is strictly local [3]. By using the decomposition

$$\frac{\delta^2 E_{\text{Hxc}}^{\text{srLDA},\mu}[n]}{\delta n(\mathbf{r}') \delta n(\mathbf{r})} = w_{\text{ee}}^{\text{sr},\mu}(|\mathbf{r} - \mathbf{r}'|) + \frac{\partial^2 e_{\text{xc}}^{\text{sr},\mu}(n(\mathbf{r}))}{\partial n^2} \delta(\mathbf{r} - \mathbf{r}'), \quad (\text{B8})$$

the first term on the right-hand side of Eq. (B7) can be simplified as follows:

$$\begin{aligned} &\iint d\mathbf{r}' d\mathbf{r} \frac{\delta^2 E_{\text{Hxc}}^{\text{srLDA},\mu}[\tilde{n}^{\mu,w}]}{\delta n(\mathbf{r}') \delta n(\mathbf{r})} \delta \tilde{n}^{\mu,w}(\mathbf{r}') \delta \tilde{n}^{\mu,w}(\mathbf{r}) \\ &= \iint d\mathbf{r}' d\mathbf{r} w_{\text{ee}}^{\text{sr},\mu}(|\mathbf{r} - \mathbf{r}'|) \delta \tilde{n}^{\mu,w}(\mathbf{r}') \delta \tilde{n}^{\mu,w}(\mathbf{r}) \\ &\quad + \int d\mathbf{r} \frac{\partial^2 e_{\text{xc}}^{\text{sr},\mu}(\tilde{n}^{\mu,w}(\mathbf{r}))}{\partial n^2} (\delta \tilde{n}^{\mu,w}(\mathbf{r}))^2. \end{aligned} \quad (\text{B9})$$

In the GOK-DFT limit ($\mu = 0$), if the first excitation is a single excitation from the HOMO to the LUMO, the auxiliary excitation energy reduces to an orbital energy difference $\Delta \tilde{\varepsilon}^w$ whose derivative can formally be expressed, according to Eq. (B7), as

$$\begin{aligned} \frac{d\Delta \tilde{\varepsilon}^w}{dw} &= \iint d\mathbf{r}' d\mathbf{r} \frac{\delta^2 E_{\text{Hxc}}[\tilde{n}^w]}{\delta n(\mathbf{r}') \delta n(\mathbf{r})} \delta \tilde{n}^w(\mathbf{r}') \delta \tilde{n}^w(\mathbf{r}) \\ &\quad + 4 \sum_{i \leq N/2, a > N/2} \frac{1}{\tilde{\varepsilon}_i^w - \tilde{\varepsilon}_a^w} \\ &\quad \times \left(\iint d\mathbf{r}' d\mathbf{r} \frac{\delta^2 E_{\text{Hxc}}[\tilde{n}^w]}{\delta n(\mathbf{r}') \delta n(\mathbf{r})} \delta \tilde{n}^w(\mathbf{r}') \tilde{\phi}_i^w(\mathbf{r}') \tilde{\phi}_a^w(\mathbf{r}') \right)^2 \\ &\quad + w \left(\iint d\mathbf{r}' d\mathbf{r} \frac{\delta^2 E_{\text{Hxc}}[\tilde{n}^w]}{\delta n(\mathbf{r}') \delta n(\mathbf{r})} \frac{\partial \delta \tilde{n}^w(\mathbf{r}')}{\partial w} \delta \tilde{n}^w(\mathbf{r}) \right) \\ &\quad + \dots, \end{aligned} \quad (\text{B10})$$

where

$$\begin{aligned}\tilde{n}^w(\mathbf{r}) &= 2 \sum_{k=1}^{N/2-1} \tilde{\phi}_k^w(\mathbf{r})^2 + (2-w)\tilde{\phi}_{N/2}^w(\mathbf{r})^2 + w\tilde{\phi}_{N/2+1}^w(\mathbf{r})^2, \\ \delta\tilde{n}^w(\mathbf{r}) &= \tilde{\phi}_{N/2+1}^w(\mathbf{r})^2 - \tilde{\phi}_{N/2}^w(\mathbf{r})^2,\end{aligned}\quad (\text{B11})$$

and $\{\tilde{\phi}_k^w(\mathbf{r})\}_k$ are the GOK-DFT orbitals with the associated energies $\{\tilde{\epsilon}_k^w\}_k$ that are obtained within the WIDFA approximation. Note that, in practical calculations, partially occupied GOK-DFT orbitals have not been computed explicitly. Instead, we performed FCI calculations in the basis of determinants constructed from the KS orbitals.

Let us, finally, note that if the HOMO and LUMO do not overlap, the first term on the right-hand side of Eq. (B10) can be further simplified at the LDA level, according to Eq. (B9), thus leading to

$$\begin{aligned}& \iint d\mathbf{r}'d\mathbf{r} \frac{\delta^2 E_{\text{Hxc}}^{\text{LDA}}[\tilde{n}^w]}{\delta n(\mathbf{r}')\delta n(\mathbf{r})} \delta\tilde{n}^w(\mathbf{r}')\delta\tilde{n}^w(\mathbf{r}) \\ & \rightarrow \iint d\mathbf{r}'d\mathbf{r} \frac{\tilde{\phi}_{N/2}^w(\mathbf{r})^2\tilde{\phi}_{N/2}^w(\mathbf{r}')^2}{|\mathbf{r}-\mathbf{r}'|} \\ & + \iint d\mathbf{r}'d\mathbf{r} \frac{\tilde{\phi}_{N/2+1}^w(\mathbf{r})^2\tilde{\phi}_{N/2+1}^w(\mathbf{r}')^2}{|\mathbf{r}-\mathbf{r}'|} \\ & + \int d\mathbf{r} \frac{\partial^2 e_{\text{xc}}(\tilde{n}^w(\mathbf{r}))}{\partial n^2} (\tilde{\phi}_{N/2}^w(\mathbf{r})^4 + \tilde{\phi}_{N/2+1}^w(\mathbf{r})^4).\end{aligned}\quad (\text{B12})$$

APPENDIX C: SELF-CONSISTENCY EFFECTS ON THE ENSEMBLE AND AUXILIARY ENERGIES

Let n denote a trial ensemble density for which the auxiliary wave functions can be determined:

$$\hat{H}^\mu[n]|\Psi_i^\mu[n]\rangle = \mathcal{E}_i^\mu[n]|\Psi_i^\mu[n]\rangle, \quad i = 0, 1. \quad (\text{C1})$$

The resulting auxiliary ensemble density,

$$n^w[n](\mathbf{r}) = (1-w)n_{\Psi_0^\mu[n]}(\mathbf{r}) + wn_{\Psi_1^\mu[n]}(\mathbf{r}), \quad (\text{C2})$$

is then a functional of n , like the ensemble energy, which can be expressed as

$$\begin{aligned}E^{\mu,w}[n] &= (1-w)\mathcal{E}_0^\mu[n] + w\mathcal{E}_1^\mu[n] \\ & - \int d\mathbf{r} \frac{\delta E_{\text{Hxc}}^{\text{sr},\mu}[n]}{\delta n(\mathbf{r})} n^w[n](\mathbf{r}) + E_{\text{Hxc}}^{\text{sr},\mu}[n^w[n]].\end{aligned}\quad (\text{C3})$$

The converged ensemble density $\tilde{n}^{\mu,w}$ fulfills the following condition:

$$n^w[\tilde{n}^{\mu,w}] = \tilde{n}^{\mu,w}. \quad (\text{C4})$$

If we now consider variations around the trial density, $n \rightarrow n + \delta n$, the ensemble energy will vary through first order in δn as

$$\begin{aligned}\delta E^{\mu,w}[n] &= (1-w)\delta\mathcal{E}_0^\mu[n] + w\delta\mathcal{E}_1^\mu[n] \\ & - \int d\mathbf{r} \delta \left(\frac{\delta E_{\text{Hxc}}^{\text{sr},\mu}[n]}{\delta n(\mathbf{r})} n^w[n](\mathbf{r}) \right) \\ & + \int d\mathbf{r} \frac{\delta E_{\text{Hxc}}^{\text{sr},\mu}[n^w[n]]}{\delta n(\mathbf{r})} \delta n^w[n](\mathbf{r}),\end{aligned}\quad (\text{C5})$$

where, according to the Hellmann-Feynman theorem,

$$\delta\mathcal{E}_i^\mu[n] = \int d\mathbf{r} \delta \left(\frac{\delta E_{\text{Hxc}}^{\text{sr},\mu}[n]}{\delta n(\mathbf{r})} \right) n_{\Psi_i^\mu[n]}(\mathbf{r}). \quad (\text{C6})$$

Combining Eqs. (C1) and (C5) with Eq. (C6) leads to

$$\delta E^{\mu,w}[n] = \int d\mathbf{r} \left(\frac{\delta E_{\text{Hxc}}^{\text{sr},\mu}[n^w[n]]}{\delta n(\mathbf{r})} - \frac{\delta E_{\text{Hxc}}^{\text{sr},\mu}[n]}{\delta n(\mathbf{r})} \right) \delta n^w[n](\mathbf{r}). \quad (\text{C7})$$

According to Eq. (C6), the auxiliary excitation energy $\Delta\mathcal{E}^\mu[n] = \mathcal{E}_1^\mu[n] - \mathcal{E}_0^\mu[n]$ will vary through first order as

$$\begin{aligned}\delta\Delta\mathcal{E}^\mu[n] &= \iint d\mathbf{r}d\mathbf{r}' \frac{\delta^2 E_{\text{Hxc}}^{\text{sr},\mu}[n]}{\delta n(\mathbf{r}')\delta n(\mathbf{r})} \delta n(\mathbf{r}') \\ & \times (n_{\Psi_1^\mu[n]}(\mathbf{r}) - n_{\Psi_0^\mu[n]}(\mathbf{r})).\end{aligned}\quad (\text{C8})$$

We conclude from Eqs. (C4), (C7), and (C8) that variations δn around the converged ensemble density $\tilde{n}^{\mu,w}$ will induce at least first- and second-order deviations in δn for the auxiliary excitation and ensemble energies, respectively.

[1] M. Casida and M. Huix-Rotllant, *Annu. Rev. Phys. Chem.* **63**, 287 (2012).
 [2] K. Pernal, *J. Chem. Phys.* **136**, 184105 (2012).
 [3] E. Rebolini, A. Savin, and J. Toulouse, *Mol. Phys.* **111**, 1219 (2013).
 [4] E. Fromager, S. Knecht, and H. J. Aa. Jensen, *J. Chem. Phys.* **138**, 084101 (2013).
 [5] E. D. Hedegård, F. Heiden, S. Knecht, E. Fromager, and H. J. Aa. Jensen, *J. Chem. Phys.* **139**, 184308 (2013).
 [6] E. K. U. Gross, L. N. Oliveira, and W. Kohn, *Phys. Rev. A* **37**, 2805 (1988).

[7] E. K. U. Gross, L. N. Oliveira, and W. Kohn, *Phys. Rev. A* **37**, 2809 (1988).
 [8] K. Andersson, P.-Å. Malmqvist, and B. O. Roos, *J. Chem. Phys.* **96**, 1218 (1992).
 [9] C. Angeli, R. Cimraglia, S. Evangelisti, T. Leininger, and J. P. Malrieu, *J. Chem. Phys.* **114**, 10252 (2001).
 [10] C. Angeli, R. Cimraglia, and J.-P. Malrieu, *J. Chem. Phys.* **117**, 9138 (2002).
 [11] A. Nikiforov, J. A. Gamez, W. Thiel, M. Huix-Rotllant, and M. Filatov, *J. Chem. Phys.* **141**, 124122 (2014).
 [12] M. Filatov, *WIREs Comput. Mol. Sci* **5**, 146 (2015).

- [13] E. Pastorzak, N. I. Gidopoulos, and K. Pernal, *Phys. Rev. A* **87**, 062501 (2013).
- [14] O. Franck and E. Fromager, *Mol. Phys.* **112**, 1684 (2014).
- [15] Z.-h. Yang, J. R. Trail, A. Pribram-Jones, K. Burke, R. J. Needs, and C. A. Ullrich, *Phys. Rev. A* **90**, 042501 (2014).
- [16] A. Pribram-Jones, Z.-h. Yang, J. R. Trail, K. Burke, R. J. Needs, and C. A. Ullrich, *J. Chem. Phys.* **140**, 18A541 (2014).
- [17] T. Stein, J. Autschbach, N. Govind, L. Kronik, and R. Baer, *J. Phys. Chem. Lett.* **3**, 3740 (2012).
- [18] P. Hohenberg and W. Kohn, *Phys. Rev.* **136**, B864 (1964).
- [19] E. H. Lieb, *Int. J. Quantum Chem.* **24**, 243 (1983).
- [20] A. Savin, *Recent Developments and Applications of Modern Density Functional Theory* (Elsevier, Amsterdam, 1996), p. 327.
- [21] J. Toulouse, A. Savin, and H. J. Flad, *Int. J. Quantum Chem.* **100**, 1047 (2004).
- [22] J. Toulouse, F. Colonna, and A. Savin, *Phys. Rev. A* **70**, 062505 (2004).
- [23] E. Goll, H. J. Werner, and H. Stoll, *Phys. Chem. Chem. Phys.* **7**, 3917 (2005).
- [24] E. Goll, M. Ernst, F. Moegle-Hofacker, and H. Stoll, *J. Chem. Phys.* **130**, 234112 (2009).
- [25] J. G. Ángyán, I. C. Gerber, A. Savin, and J. Toulouse, *Phys. Rev. A* **72**, 012510 (2005).
- [26] E. Fromager, J. Toulouse, and H. J. Aa. Jensen, *J. Chem. Phys.* **126**, 074111 (2007).
- [27] E. Fromager and H. J. Aa. Jensen, *Phys. Rev. A* **78**, 022504 (2008).
- [28] J. G. Ángyán, *Phys. Rev. A* **78**, 022510 (2008).
- [29] J. Toulouse, I. C. Gerber, G. Jansen, A. Savin, and J. G. Ángyán, *Phys. Rev. Lett.* **102**, 096404 (2009).
- [30] B. G. Janesko, T. M. Henderson, and G. E. Scuseria, *J. Chem. Phys.* **130**, 081105 (2009).
- [31] T. Leininger, H. Stoll, H. J. Werner, and A. Savin, *Chem. Phys. Lett.* **275**, 151 (1997).
- [32] R. Pollet, A. Savin, T. Leininger, and H. Stoll, *J. Chem. Phys.* **116**, 1250 (2002).
- [33] E. Fromager, R. Cimraglia, and H. J. Aa. Jensen, *Phys. Rev. A* **81**, 024502 (2010).
- [34] D. R. Rohr, J. Toulouse, and K. Pernal, *Phys. Rev. A* **82**, 052502 (2010).
- [35] E. D. Hedegård, S. Knecht, J. S. Kielberg, H. J. Aa. Jensen, and M. Reiher, *J. Chem. Phys.* **142**, 224108 (2015).
- [36] A. Savin, *J. Chem. Phys.* **140**, 18A509 (2014).
- [37] E. Rebolini, J. Toulouse, A. M. Teale, T. Helgaker, and A. Savin, *J. Chem. Phys.* **141**, 044123 (2014).
- [38] E. Rebolini, J. Toulouse, A. M. Teale, T. Helgaker, and A. Savin, *Phys. Rev. A* **91**, 032519 (2015).
- [39] E. Rebolini, J. Toulouse, A. M. Teale, T. Helgaker, and A. Savin, *Mol. Phys.* **113**, 1740 (2015).
- [40] A. K. Theophilou, *J. Phys. C (Solid State Phys.)* **12**, 5419 (1979).
- [41] N. I. Gidopoulos, P. G. Papaconstantinou, and E. K. U. Gross, *Phys. Rev. Lett.* **88**, 033003 (2002).
- [42] E. Pastorzak and K. Pernal, *J. Chem. Phys.* **140**, 18A514 (2014).
- [43] M. Levy, *Phys. Rev. A* **52**, R4313 (1995).
- [44] E. Kraisler and L. Kronik, *Phys. Rev. Lett.* **110**, 126403 (2013).
- [45] E. Kraisler and L. Kronik, *J. Chem. Phys.* **140**, 18A540 (2014).
- [46] T. Gould and J. Toulouse, *Phys. Rev. A* **90**, 050502 (2014).
- [47] K. Aidas, C. Angeli, K. L. Bak, V. Bakken, R. Bast, L. Boman, O. Christiansen, R. Cimraglia, S. Coriani, P. Dahle, E. K. Dalskov, U. Ekström, T. Enevoldsen, J. J. Eriksen, P. Ettenhuber, B. Fernández, L. Ferrighi, H. Fliegl, L. Frediani, K. Hald, A. Halkier, C. Hättig, H. Heiberg, T. Helgaker, A. C. Hennum, H. Hettema, E. Hjertenæs, S. Høst, I.-M. Høyvik, M. F. Iozzi, B. Jansík, H. J. Aa. Jensen, D. Jonsson, P. Jørgensen, J. Kauczor, S. Kirpekar, T. Kjærgaard, W. Klopper, S. Knecht, R. Kobayashi, H. Koch, J. Kongsted, A. Krapp, K. Kristensen, A. Ligabue, O. B. Lutnæs, J. I. Melo, K. V. Mikkelsen, R. H. Myhre, C. Neiss, C. B. Nielsen, P. Norman, J. Olsen, J. M. H. Olsen, A. Osted, M. J. Packer, F. Pawłowski, T. B. Pedersen, P. F. Provasi, S. Reine, Z. Rinkevicius, T. A. Ruden, K. Ruud, V. V. Rybkin, P. Salek, C. C. M. Samson, A. S. de Merás, T. Saue, S. P. A. Sauer, B. Schimmelpfennig, K. Sneskov, A. H. Steindal, K. O. Sylvester-Hvid, P. R. Taylor, A. M. Teale, E. I. Tellgren, D. P. Tew, A. J. Thorvaldsen, L. Thøgersen, O. Vahtras, M. A. Watson, D. J. D. Wilson, M. Ziolkowski, and H. Ågren, *WIREs Comput. Mol. Sci.* **4**, 269 (2015).
- [48] Dalton, a molecular electronic structure program, Release Dalton2015 (2015); <http://daltonprogram.org>.
- [49] T. H. Dunning, *J. Chem. Phys.* **90**, 1007 (1989).
- [50] D. E. Woon and T. H. Dunning, *J. Chem. Phys.* **100**, 2975 (1994).
- [51] S. H. Vosko, L. Wilk, and M. Nusair, *Can. J. Phys.* **58**, 1200 (1980).
- [52] J. P. Perdew, K. Burke, and M. Ernzerhof, *Phys. Rev. Lett.* **77**, 3865 (1996).
- [53] T. Yanai, D. P. Tew, and N. C. Handy, *Chem. Phys. Lett.* **393**, 51 (2004).
- [54] P. Gori-Giorgi and A. Savin, *Int. J. Quantum Chem.* **109**, 1950 (2009).
- [55] E. Fromager, *Mol. Phys.* **113**, 419 (2015).
- [56] O. Franck, B. Mussard, E. Luppi, and J. Toulouse, *J. Chem. Phys.* **142**, 074107 (2015).